FABRICATION, CHARACTERIZATION AND BUFFER LAYER MODIFICATION OF P3HT: PCBM BASED ORGANIC SOLAR CELLS

A DISSERTATION SUBMITTED TOWARDS THE PARTIAL FULFILLMENT OF THE REQUIREMENT FOR THE AWARD OF DEGREE OF

MASTER OF TECHNOLOGY

IN

NANOSCIENCE AND TECHNOLOGY

SUBMITTED BY

SONAL PARAKH

(ROLL NO. 2K11/NST/15)

UNDER THE SUPERVISION OF

Dr. SURESH CHAND (EXT. SUPERVISOR-I, NPL)

Dr. J. P. TIWARI (EXT.SUPERVISOR-II, NPL)

Dr. NITIN PURI (INT. SUPERVISOR,DTU)

DEPARTMENT OF APPLIED PHYSICS

DELHI TECHNOLOGICAL UNIVERSITY

(FORMERLY DELHI COLLEGE OF ENGINEERING)

CERTIFICATE-II

This is to certify that **Ms. Sonal Parakh** (2K11/NST/15) has carried out the major project titled "**FABRICATION, CHARACTERIZATION AND BUFFER LAYER MODIFICATION OF P3HT:PCBM BASED ORGANIC SOLAR CELLS**" as a partial requirement for the award of Master of Technology degree in Nanoscience and Technology by Delhi Technological University. The matter contained in this report has not been submitted elsewhere for the award of any other degree.

Prof. S.C. Sharma
HOD, Dept. of Applied Physics
Delhi Technological University
Delhi-110042

Dr. Nitin K. Puri
Assistant Professor
Delhi Technological University
Delhi-110042

DECLARATION BY THE CANDIDATE

I hereby declare that the work presented in this dissertation entitled "**FABRICATION, CHARACTERIZATION AND BUFFER LAYER MODIFICATION OF P3HT:PCBM BASED ORGANIC SOLAR CELLS**" has been carried out by me under the guidance of external supervisors Dr. Suresh Chand and Dr. J. P. Tiwari, National Physical Laboratory and internal supervisor Dr. Nitin K. Puri, Assistant Professor, Department of Applied Physics, Delhi Technological University, Delhi and is hereby submitted for the partial fulfillment for the award of degree of Master of Technology in Nanoscience and Technology at Applied Physics Department, Delhi Technological University, Delhi.

I further undertake that the work embodied in this major project has not been submitted for the award of any other degree elsewhere.

Sonal Parakh

Roll no- 2K11/NST/15

M.Tech

(Nanoscience and Technology)

Delhi Technological University

ACKNOWLEDGEMENT

I express my deep sense of gratitude to **Dr. Suresh Chand** who was my supervisor for providing me an opportunity to work in Organic and Hybrid Solar Cell Section, NPL. His wide knowledge, logical way of thinking and pitch-perfect instincts on all matters large and small have been of great value to me. I want to express my deep sense of gratitude to my supervisor **Dr. J.P. Tiwari** who was my co-guide in NPL. His constructive criticism and insight was necessary without which the project would not have shaped as it has.

I express my gratitude to **Prof. S.C. Sharma**, Head of Department, Department of Applied Physics, Delhi Technological University, Delhi and **Dr. Nitin K. Puri** who was my guide and branch coordinator. Their invaluable support and encouragement was very vital towards completing this thesis.

I would like to acknowledge all members of Organic and Hybrid Solar Cell Section at NPL for their kind support in my work, with very special thanks to senior research fellow **Mr. Abhishek Sharma** and **Mr. Neeraj Chaudhary** for their everlasting support and efforts. Words cannot express my gratefulness to them for providing their valuable help and time whenever required.

I also want to thank my classmates at Delhi Technological University, Delhi and in particular **Ms. Prashansa Dalal** and **Mr. Sriraj Pillai**. I never could have thought that research could be this fun with you two around.

I take pride of myself being the son of ideal parents for their everlasting desire, sacrifice, affectionate blessings, and help, without which it would not have been possible for me to complete my studies.

Last but not the least my loving grandparents have been very keen on my completing this work. Their encouragement and blessings made it possible for me to achieve this.

Sonal Parakh

Roll No. 2K11/NST/15

M.Tech (Nanoscience and Tech.)

E-mail: sonalparakh22@gmail.com

Abstract

Concerns about Global Warming and diminishing fossil fuel reserves have accelerated the search for low cost sources of renewable energy. Organic photovoltaics (OPVs) could be one such source. This thesis took the first step towards that goal by developing a process to synthesize and characterize inverted and normal poly (3-hexylthiophene) (P3HT), [6,6]-phenyl-C61 butyric acid methyl ester ($PC_{60}BM$) solar cells. Although detrimental to the stability of the cells, ambient synthesis replicated the conditions required for large-scale, industrial production.

Performance and stability were evaluated for each type of OPV. The most efficient normal cell had a power conversion efficiency of 0.308 %, a fill factor of 32.8%, and a V_{OC} of up to 0.557 V. The buffer layer used was replaced by new transition oxides (MoO_3) due to the limitations faced by the traditional layers. Then, some new inverted structures were investigated with efficiencies as high as 1.71 %, with a fill factor of 58.2 % and a V_{OC} of 0.606 V. The inverted cells were much more stable than the normal cells. Some cells with new polymers need optimization but they did give some promising results.

CONTENTS

1. Introduction

2. Theory and Characterization

3. Structure, Materials and Techniques

4. Organic Solar Cell Fabrication

1. **INTRODUCTION**

1.1 Energy consumption

The ever increasing demand of energy on earth and the contrasting over exploitation of the available fossil fuels, resulting in their growing shortage as well as an increased emission of greenhouse gasses altering the energy balance of the climate system with unforeseen consequences for the planet, has forced us to look for a more dependable, sustainable and feasible alternative to meet our energy demands.

It might be asked if renewable energy is so beneficial, why don't we consume more of it? The answer is that most of the renewable energy sources are little difficult to harvest and retrieve. Thus, because of these limitations, our interest has always been towards the then largely available and hence an obvious choice - fossil fuels. But, Fossil fuels are non-renewable and are limited, which are dwindling because of their high cost and environmentally damaging retrieval techniques. So, the need for renewable, less expensive and eco friendly resources and the scope for their research and development is rising by the day.

Since a return to a pre-industrial era is impossible, and we are heading towards development for making the world a better place to live in, renewable energy (wind, solar, hydroelectric, geothermal, or nuclear) will have to supply a significant portion of our power.

Table 1: Energy available for harvesting from different sources compared to the global energy demand [8, 9].

Global consumption	Hydro	Geothermal	Wind	Solar
15 TW	7.2 TW	32 TW	870 TW	86,000 TW

As shown above in the Table 1.1, we can clearly see that one of the most efficient of all these renewable sources is solar energy which is a lot more than the global consumption. So, the potential of solar power is limitless. In 2011, according to International Energy Agency, one-third of the world’s energy demand could be met by solar power given that the climatic conditions must be kept under good consideration.

1.2 The Importance of Solar Energy

If solar energy could replace our conventional fossil fuels, our environment would be benefited by that the most. It would reduce air pollution as solar energy does not contributes to produce excessively injurious pollutants that are liable for the greenhouse effect which in turn gives rise to global warming. It isn't hard to believe that somehow the fossil fuels contribute to the cause of global warming, which will ultimately result in the demise of our planet. So, solar energy being a renewable resource would stay there forever i.e. it will be consumed by all practical human usages. Fossil fuels like coal, oil etc, are all limited and would soon end as it seems by the pace with which we are exploiting them. So our aim should be to save them as much as we can and use better alternatives that are not near their end like the fossil fuels.

If we wish to prevent an environmental catastrophe we require an end to the fossil fuel addiction, a challenge for our generation. A panel of scientists assembled by United Nations highlighted the major threats posed by green house gases. The Intergovernmental panel on Climate Change stated that the maximum atmospheric CO_2 concentration could be 450ppm i.e. beyond this threshold value, drastic climatic changes would likely be inevitable. The average atmospheric CO2 concentration in 2009 was 387 ppm [1], which according to some scientists is already past a safe threshold of 350 ppm [2].

Solar energy provides future energy security by reducing the need for foreign fuel import and being a growing field in the energy development it can also provide new jobs and career opportunities for our youth. Fig. 1.1 gives a schematic diagram showing the percentage distribution of solar energy which gives us an idea of how much energy is reflected back and the surplus energy left to be utilised and harvested as one of the strongest energy resource.

The best thing about solar energy is, it is free to use as nobody owns the sun. The only challenge for human race is to be able to harness as much energy of the sun as we can by various means and types of solar power plants that are being designed and proposed. The amount of energy Earth receives from sun is as good as 174 petawatts at the upper atmospheric layers, 30% of which is reflected back into space which still leaves almost 4 million exajoules (almost 51%) per year reaching the land masses and oceans – 10,000 times the global power consumption.

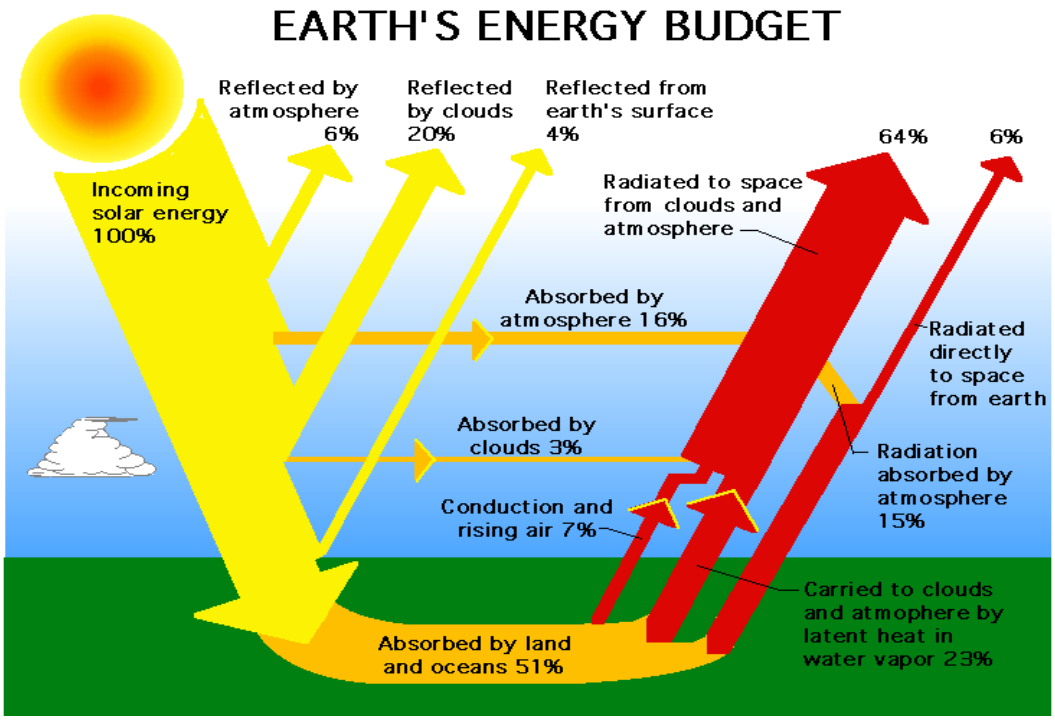

Figure 1.1: Flow diagram showing the distribution of solar radiation falling on Earth.

All this enables us to state that this huge amount can easily surpass the amount of energy obtained by all non-renewable resources of coal, oil, natural gas, and mined uranium in less than a year. In 2008, solar energy covered a small portion of the nation's energy, about 0.1% of total energy and 2% of renewable energy [3]. But this was more energy in 1 hour than the world used in 1 year in the year 2002. This small but considerable market share is due to the result of highly efficient research and implementation of solar cell technology. This thesis is also directed to the same that is the study of conversion of solar radiation into electrical energy through photovoltaics [4].

1.3 Types of Solar Cells

Solar cells can be best classified in terms of generations i.e. the development and variations in solar cells with time.

So far there have been three such generations of solar cells as follows:

1.3.1 First Generation

First generation photovoltaics include single PN junction silicon solar cells. This category of solar cells is the most commercialised one covering 90% of the photovoltaic market. [5]

The most important parameter of the performance of a solar cell is its Power conversion efficiency (PCE), i.e. the percent of incoming solar radiation that is converted to usable power by the solar cell. So far, the highest theoretical efficiency that is reported by Shockley and Queissier i.e. 33% for any type of single cell solar cell with a band gap of 1.1 eV. [6] On the other hand Kerr et al. calculated that for a 90μm thick single junction solar cell to be 29%. [7]

For a solar cell to operate, the light reaching the earth has to be energetic enough to excite the electrons over the band gap. So semiconductor bandgap is one of the greatest parameter while choosing the semiconductor for photovoltaic cells because that determines how much energy the incoming solar radiation has to offer in order to excite the electrons. For this mostly short wavelength or ultraviolet radiations proves beneficial that generates lattice vibrations known as phonons.

(a) Monocrystalline Silicon Cells

Solar cells made from thin wafers of silicon are the most prominent solar cell technology even today in spite of being the oldest. These cells are sliced from large single crystals that have been grown in a controlled environment with tremendous efforts and hence called as monocrystalline solar cells. A panel is made up of a number of cells laid out in a grid and are a few inches across (Fig. 1.2).

They have a higher efficiency (up to 24.2%) as compared to other types of cells which means that more electricity can be produced from a given panel area [8]. But, this approach has its own disadvantage of being economically incompetent as growing large crystals of pure silicon is a very tedious and energy intensive process.

(b) Polycrstalline Silicon Cells

The production of silicon wafers in moulds from multiple silicon crystals rather than from a single crystal is obviously cheaper and easier as compared to the production of monocrystalline solar cells, as the growing environment need not be as controlled and specific. A number of silicon crystals are grown together to make polycrystalline solar cells. No doubt panels on these cells are cheaper per unit area but they suffer in efficiency (up to 19.3%).

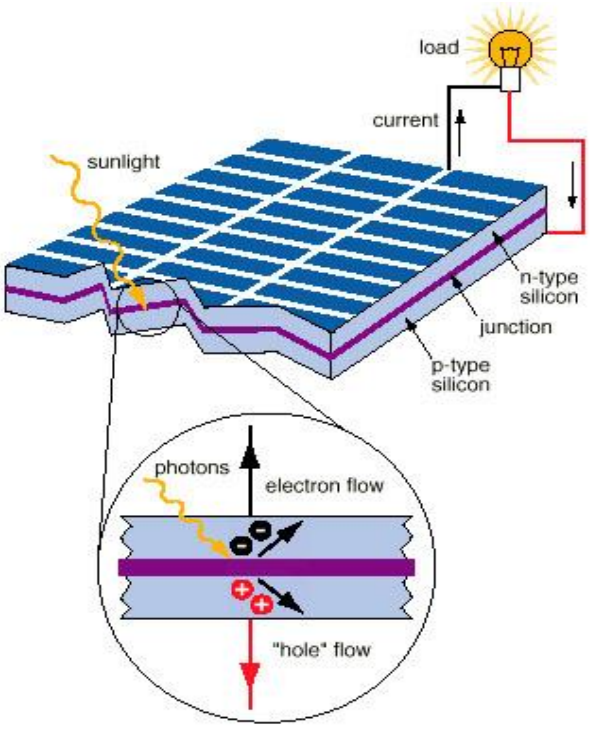

Figure 1.2: A basic schematic diagram for first generation solar cells.

(c) Amorphous Silicon Cells

In amorphous silicon cells of cells silicon crystals are not grown as is done in the previous two types, instead silicon is deposited in a very sleek layer on a backing substrate such as metal, glass, or plastic. In these cells various silicon layers are mixed with impurities accordingly to respond to various wavelengths of light and are laid in a stack to improve efficiency. The production methods are complex but less energy intensive as compared to crystalline panels, and as the panels are mass-produced the prices are coming down as the tedious process of creation of crystals is not there. One advantage of using very thin layers of silicon in panels is their flexibility, second their performance in low light levels, and the last is their efficiency maintenance as the temperature increases.

(d) Hybrid Silicon Cells

As the name suggests the origin of this type of silicon solar cells was after exploring ways of combining different materials to make a hybrid with better efficiency, stability at reduced costs. Recently introduced hybrid HIT cell consisted of a layer of amorphous silicon over single crystal wafers. It was found that the efficiency improved and even stabilised with fluctuations in temperature of the place.

First generation solar cells have highest efficiencies and lifetimes among all other types. The only limitation it faces is its high production cost that prevents them from being economically competitive and hence open doors for other research domains. In August 2010, Solar buzz, an international solar energy research and consulting firm, confirmed the residential price per kilowatt-hour of solar electricity was approximately 35 cents [9]. Despite of a considerable fall in the manufacturing costs of these solar cells, the question that still remains is how far the prices can still be reduced. Also, the increasing demand for microprocessors and other silicon-requiring devices are adding to the concern that whether these prices are going to fall in near future or not.

1.3.2 Second Generation

The cost related limitations of the first generation solar cells has shifted the focus of the researchers on the development of more cost effective second generation thin film solar cells [10]. The trick behind the reduction in costs of these solar cells lies in the use of less material for their generation. The thin films are only a few micrometers thick i.e. much less than the crystalline silicon based cells. So use of less material and lower manufacturing costs enables manufacturers to produce and hence sell panels at a comparatively much lower cost.

The second generation includes amorphous silicon (mentioned above) and two more that are made up of non-silicon materials – cadmium telluride (CdTe) and copper indium gallium di selenide (CIGS). These solar cells are fabricated by sputtering, physical vapour deposition, and plasma-enhanced chemical vapour deposition. The highest recorded efficiency is as good as 19.6% [8], which is not very far from the crystalline silicon results. This combination of moderately high efficiency and low manufacturing costs makes the second generation solar cells a good area of interest for the researchers.

1.3.3 Third Generation

This generation marked a completely new era in the development of solar cells giving birth to a totally new direction of research and development, i.e. organic photovoltaics(IPVs), dye-sensitized cells (DSCs), and multijunction cells. This approach was also an effort to bring down the costs of solar cells further.

Organic photovoltaics use polymers for light absorption and even for the PN junction with highest recorded efficiency to be 9.2% [11]. These not so favourable efficiencies can however be compensated by their low costs [12].

On the other hand the multijunction solar cells aim at maximising the efficiency and thereby reducing the relative cost or increasing power to cost ratio. These cells contain multiple cells, with different band gaps, stacked over one another so that they can capture maximum region of solar radiation spectrum. A specific combination of the stack can be made to perfectly match the spectrum and result in the efficiency that can even exceed that reported by Shockley and Queisser. The theoretical efficiency limit has reached up to 66% [13]. The laboratories have already witnessed 40% for triple- junction stacked PVs. In 2008, the National Renewable Energy Laboratory (NREL) reported a world record efficiency for a thin triple-junction gallium indium phosphide and gallium indium arsenide cell to be 41.6% [8] (Fig. 1.3). It reported the main milestones achieved in various solar cell technologies along with their respective year.

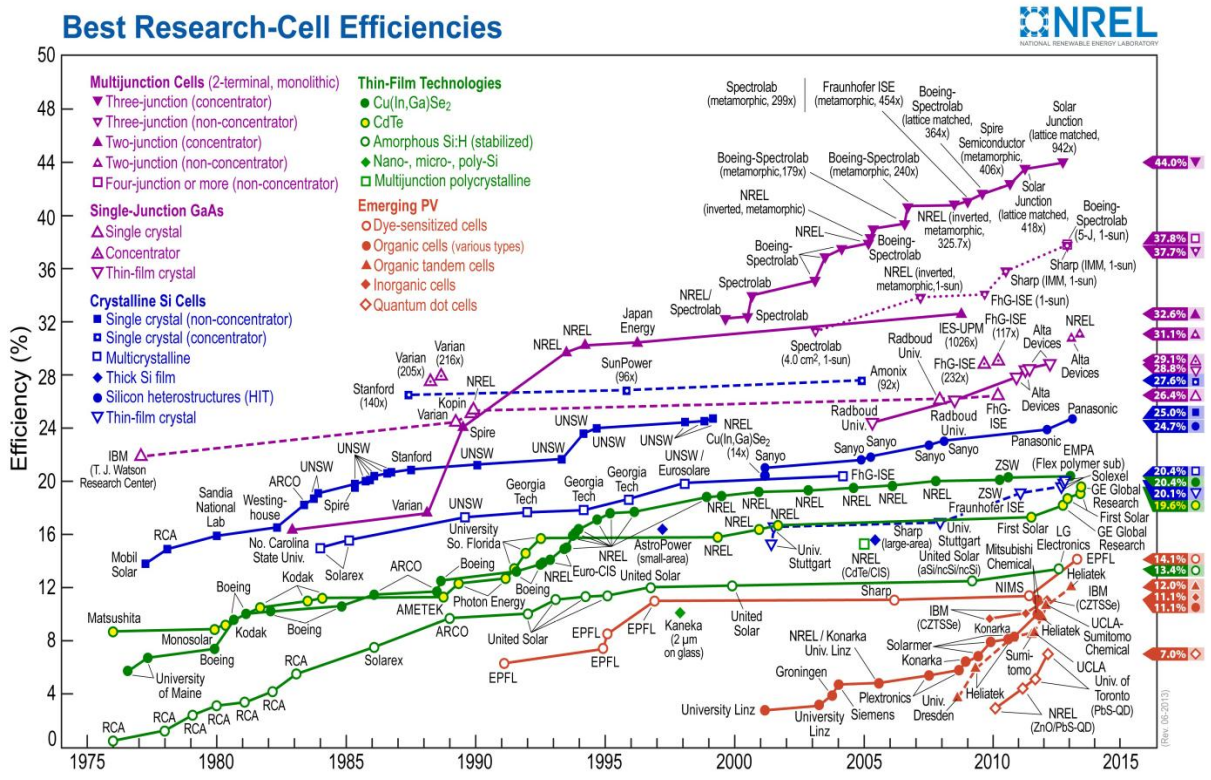

Figure 1.3: The highest recorded efficiencies of a variety of photovoltaic cells [14].

A major obstacle is the relatively high production cost of silicon-based technology when compared to other sources of energy. The fabrication of inorganic devices requires intensive processing at high temperatures as well as high vacuum conditions and requires a large number of lithographic steps. Solar cells are therefore not widely used for commercial electricity production because they cannot compete with fossil fuels or other renewable

energy sources as seen in (Figure 1.4). Therefore, in order to fully explore the potential of photovoltaic technology, new materials have to be developed.

Introduction of polymers to solar cells is a promising candidate for low manufacturing cast of solar cells [15]. Their solubility means that they are easy to process. Polymer solar cells have been studied intensively in recent years. The present power conversion efficiency (PCE) of bulk heterojunction (BHJ) based polymer solar cells has exceeded 9% [11], but it is still much below the value for inorganic solar cells, and in addition, their lifetime is significantly shorter. However, organic photovoltaic technology shows great promise for decreasing the cost of solar energy. The semiconducting materials that comprise the active layer are polymers or small molecules, which potentially are much cheaper to prepare and process than inorganic materials thanks to straight forward fabrication method such as roll-to-roll (R2R) print. Furthermore, this technology offers the possibility for thin, flexible, lightweight devices due to the superior mechanical characteristics of many organic materials; especially polymers.

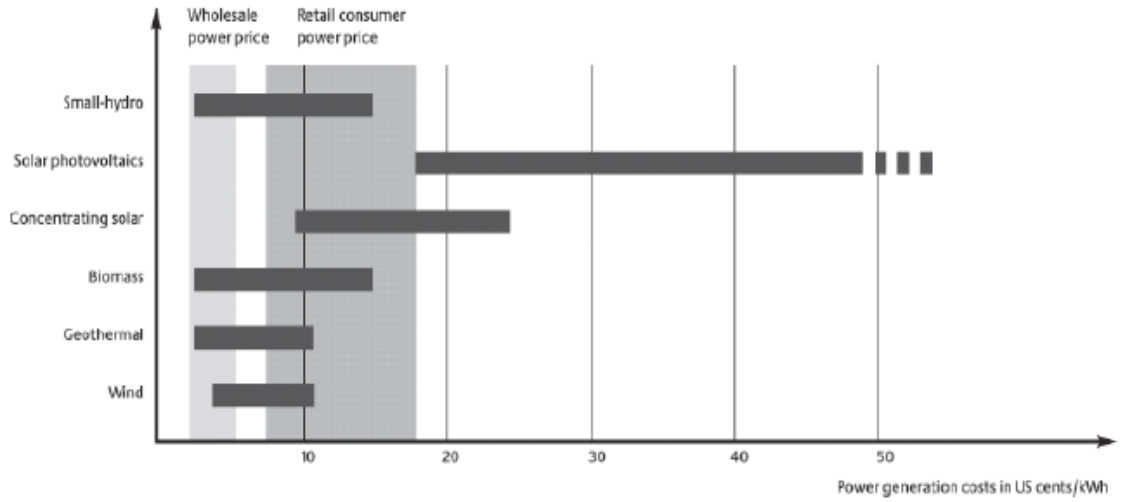

Figure 1.4: Prices of electricity produced from different renewable energy sources [16].

1.4 Organic Photovoltaics

1.4.1 Importance

Organic photovoltaics are solar cells that use organic materials like polymers (macromolecules) or small molecules. The conjugated polymers combine the advantageous properties of the conventional semiconductors with the comfort of processing and mechanical flexibility of plastics. Hence, this plastic solar cell technology has managed to attract

attention in the past few years with the promise of providing environment friendly, flexible, light weighted, inexpensive, efficient solar cells.

The cost reduction of OPVs is mainly due to the solution route, i.e. it employs soluble polymers, and since plastics have high absorption coefficient, very small quantity of material is needed [17]. Their solubility enables one to use wet-processing techniques like spin coating or roll-to-roll printing (Fig. 1.5). Another advantage is that as they are not crystalline in nature, they can be deposited on flexible substrates. In Denmark, Krebs et al. demonstrated one potential application of pliable photovoltaics at a music festival [18].

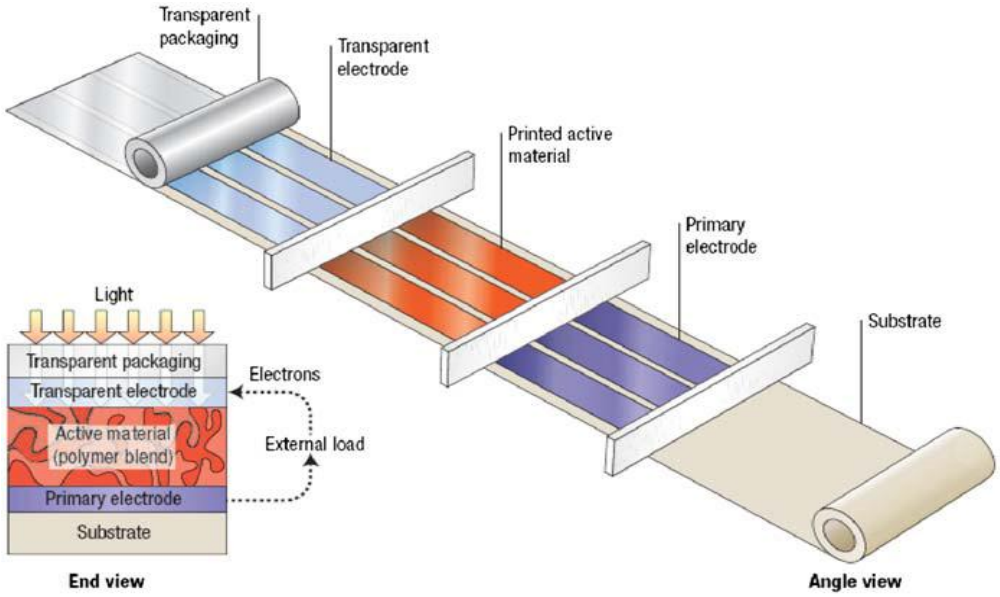

Figure 1.5: Schematic illustration of standard printing processes in polymer solar cells [19].

1.4.2 Operational Overview

In the organic solar cells, the free charge carriers are generated when sunlight falls on the organic material as shown in Fig. 1.6.

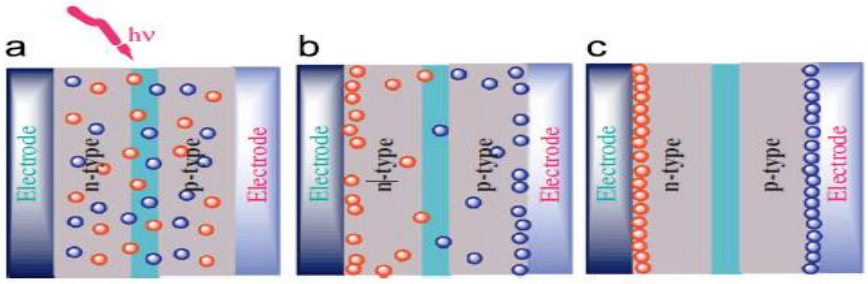

Figure 1.6: Schematic illustration of operational mechanisms in polymer solar cells. (a)Absorption of light, (b)charge separation and (c)charge collection. [20]

In order to achieve efficient collection of photons, the absorption spectrum of the photoactive polymer should coincide with the solar emission spectrum as much as possible. Hence, this demands a low band gap of the organic material which will on the contrary have some bearing on the open-circuit voltage. On the other hand increasing the layer thickness improves the light absorption but affects the charge transport negatively. Keeping these factors in mind, various methodologies have been employed for construction of organic solar cells.

1.4.3 Different approaches towards OPVs

Many different approaches have been successfully employed to produce different types of OPVs.

(a) Dye-sensitized Solar Cells

First in this category is dye-sensitized solar cell (DSSC) which consists of an organic dye absorbed at the surface of an inorganic wide gap semiconductor. They gained much attention after Brian O'Regan and Michael Grätzel improved the interfacial area between the organic donor and inorganic acceptor using nanoporous titanium dioxide (TiO_2) (Fig.1.7) [21]. The highest efficiency achieved for this type of solar cell is for a ruthenium dye-sensitized nanocrystalline TiO_2 and that is almost 10%. [22].

(4)

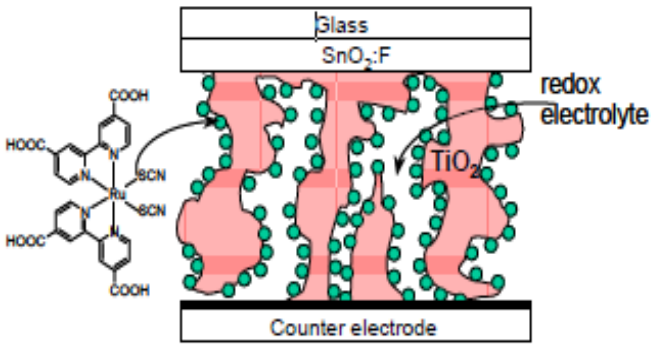

Figure 1.7: The dye-sensitized solar cell.

(b) Double Layer Cells

The first organic solar cells were made by inserting a single organic layer in between two dissimilar electrodes.

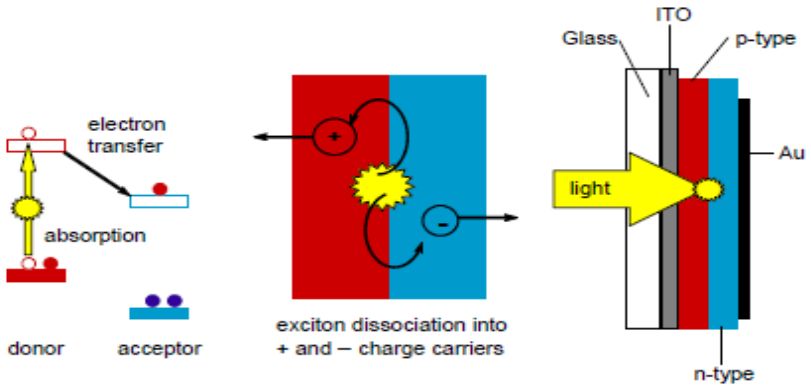

Figure 1.8: Schematic diagram of the working principle of an organic photovoltaic cell [23].

The photovoltaic results of these cells depended on the level of doping that resulted with PCEs up to 0.3% [24].

In this structure (Fig.1.8), the photoexcitations have to reach the interface of the p-n junctions where they undergo charge separation, before losing the requisite energy. As the exciton diffusion length of the organic material is mostly limited to 5-10nm [25], the layer has to be very thin for light absorption. This low thickness in turn affects its photon absorption capability. Hence, in order to improve the efficiency, focus has been shifted to structural organization of the organic material to increase its diffusion length which could enable one to create thicker layers for good absorption as well.

(c) Bulk Heterojunction Cells (BHJ)

All the above mentioned generations of solar cells have relatively high production cost of silicon based technology. The fabrication of inorganic devices requires intensive processing at high temperatures as well as high vacuum conditions and requires a large number of lithographic steps. Solar cells are therefore not widely used for commercial electricity production because they still need to go a long way before they could compete with other renewable energy sources. Thus, we adopt this BHJ approach. The power conversion efficiency of BHJ polymer solar cells has reached up to 9.2% [11], which is still much below that of Si solar cells along with not so good lifetime either. But the challenge that this solar cell technology fights is its ability to fabricate low cost devices. Due to the use of organic

materials as the semiconducting material and the easy processing techniques like spin coating, roll to roll print etc, they are relatively much cheaper. It also enables to design thin, flexible, lightweight devices due to extraordinary mechanical properties of the polymers.

So, this is the approach that would remain our main concern in this thesis work. When the p-type and n-type layers are combined together forming the p-n junction in the active layer, the greatest concern is that the excitons so generated diffuse to the interface to allow charge separation. But due to their low mobility and short lifetime, the diffusion length is just restricted to ~10nm. So, this demands that for efficient charge generation the distance between the interface and the charge generation site must be of the order of the diffusion length of the exciton. This means that the exciton has to reach a nearest donor-acceptor interface within a few nanometer otherwise it will be lost without charge generation. It was found that even a 20nm thick layer of the active materials was not sufficient enough for efficient photon absorption. So on one hand a thick layer would interrupt the charge separation due to short diffusion lengths of excitons and on the other a thin layer would affect the photon absorption. This dilemma was then dealt with a new approach of manufacturing solar cells i.e. by mixing the p and n type materials and letting the polymers create junctions throughout the bulk of the material, hence ensuring quantitative dissociation.

The first initiative to take benefit of this new bulk heterojunction approach was Polymer-fullerene solar cells (Fig.1.9) [26]. The challenge that this new solution had to face was to enable a smooth and effective migration of charge carriers towards their respective electrodes. So, these layers should be mixed into a bi-continuous network in which the inclusions or barrier layers are avoided.

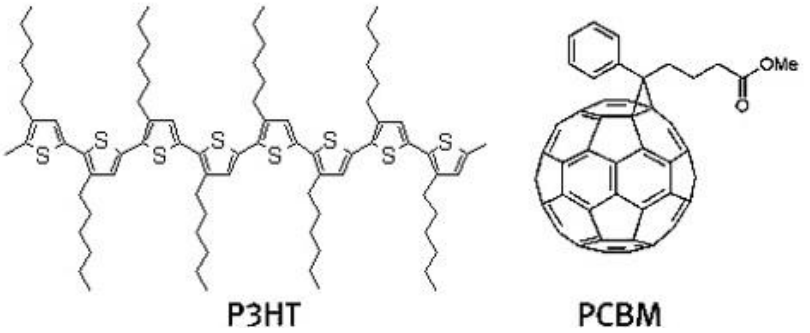

Figure 1.9: The polymer poly (3-hexylthiophene) (P3HT) and the fullerene [6,6]-phenyl-C61 butyric acid methyl ester (PCBM) [27]

A schematic illustration of the solar cell of this type is shown in figure 1.10. In this type, the interface or the heterojunctions are all over the surface or the bulk, hence the name bulk heterojunction.

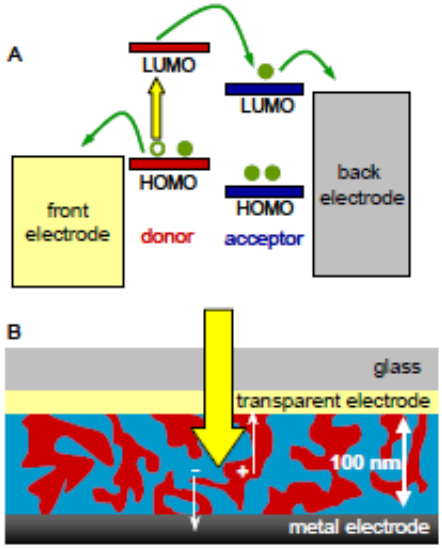

Figure 1.10: The bulk heterojunction approach. When the photons are incident over the photoactive material, charge transfer occurs due to the mixing of the donor and acceptor material (blue and red area). The generated charges are then transported and collected at the respective electrodes [23].

The role of the photoactive layers with the combination mentioned above is quite overwhelming. At their interfaces there occurs a sub-picosecond charge transfer that leads to efficient charge generation. The lifetimes of the chare separated state extends n these blends hence ensuring an effective diffusion of the generated carriers away from the interface towards the electrodes.

1.4.4 Possible routes for improving performance

(a) Stability and Lifetime

This new range of polymer based solar cells are required to undergo the stability test i.e. how stable they are when it comes to the degradation caused by the surrounding conditions. The active layers are prone to air as well as light, on the other hand the electrodes needs to be protected from oxygen and water (Fig.1.11).

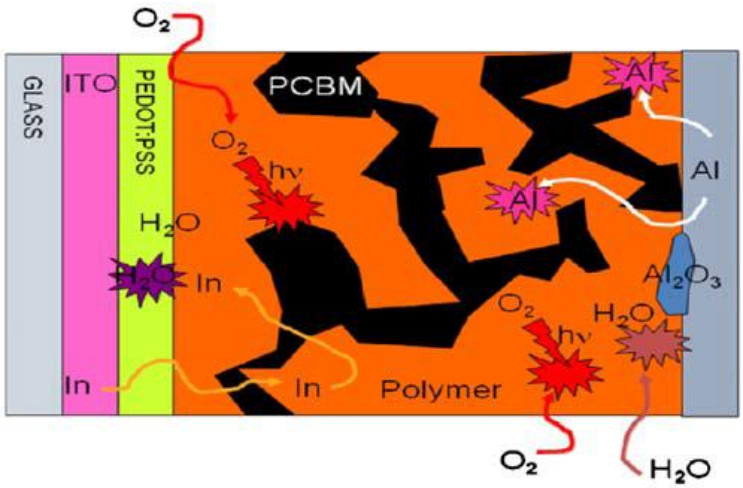

Figure 1.11: A graphical overview of the field of stability and degradation of polymer solar cells. [28].

Another prominent degradation pathway was found to be the diffusion of electrode materials into the devices. The degradation is also due to the change of the interface of the devices. Krebs and Norrman [29] observed that indium was diffused in the layer in an OPV with a structure of Al/C60/P3CT/ITO, P3CT being poly (3-carboxythio-phene-co-thiophene). Kawano et al. [130] also found that the resistance of ITO was increased due to the hygroscopic PEDOT:PSS layer absorbed the moisture from the ambient atmosphere.

(b) New Device Structures

It has been proven that acidic PEDOT:PSS layer was detrimental to active polymer layer, and the low work function metal cathode was easily to be oxidized in air even with a delicate encapsulation. Polymer solar cells with an inverted structure were discovered to overcome above shortages. Takanezawa et al. [30] reported an inverted cell structure by introducing a ZnO nanorod layer between ITO electrode and active layer. The ZnO nanorods work as the electron collectors by shortening the average electron diffusion distance in the PCBM net work in the bulk heterojunction. The ZnO nanorods also work as direct paths to transport charge carrier to the ITO electrode, resulting in a decreased charge recombination. Therefore, a larger FF was observed. This motivates one to further investigate the use of different nanocomposites along with ZnO in order to improvise the surface morphology and better contacts between various interlayers of the OSCs.

2. THEORY and CHARACTERIZATION

2.1 Inorganic Photovoltaic Cell:

When light falls on the p-n junction of an inorganic photovoltaic cell, it leads to the formation of free charge carriers. A p-n junction is a simple interface between a p type (excess holes) and n type (excess electrons) semiconductor (Fig.2.1). A p type semiconductor can be formed by diffusing boron (three valance electrons or trivalent) into silicon. This causes the generation of positive (hole or a vacancy) carriers throughout the lattice. N type semiconductor can be formed by doping phosphorous (five valence electrons or pentavalent) into the silicon wafer. This doping causes generation of excess electrons in the silicon lattice.

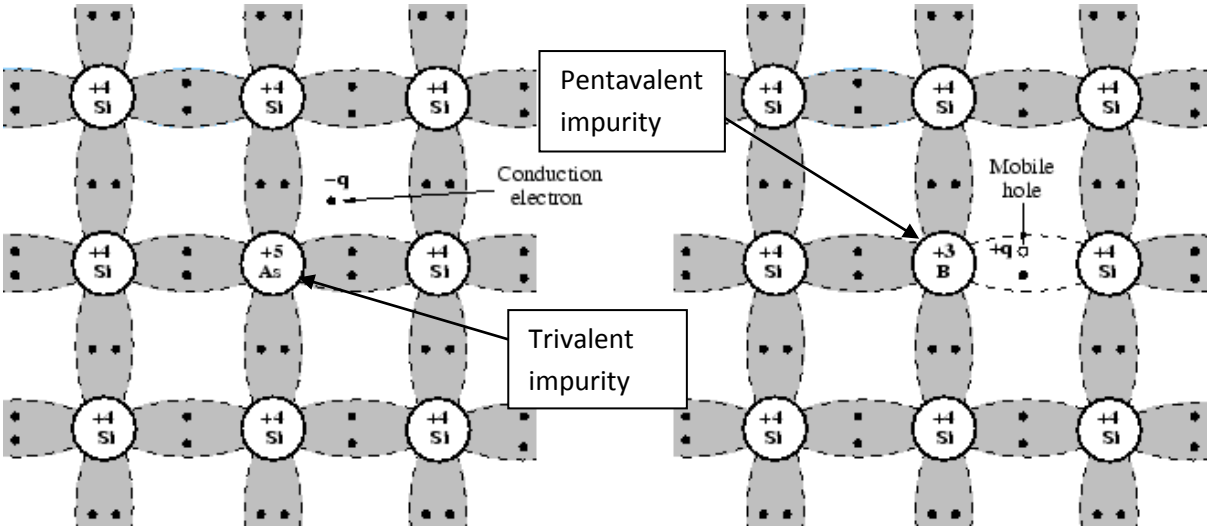

Figure 2.1: From left to right: n and p-type doping of silicon wafer.

When an N-type and P-type material are brought close to each other together to form a junction, the electrons from the N-type diffuse into the P-type and the holes from the P-type diffuse into the N-type. This leaves positive and negative ions in N-side and P-side respectively. This region is devoid of any mobile majority charge carriers (electrons and holes). Opposite charge builds up at the interface due to minority charge carriers (ions) creating an electric field that opposes the flow of electrons in this area. Hence, it is called the depletion region. This process can be visually depicted as in Fig. 2.2.

Photons coming from the sun having adequate energy excite the valence electrons from the valence band across the forbidden gap into the conduction band. Thus, these electrons being free in nature can be channelled through an external circuit before recombining thereby producing current.

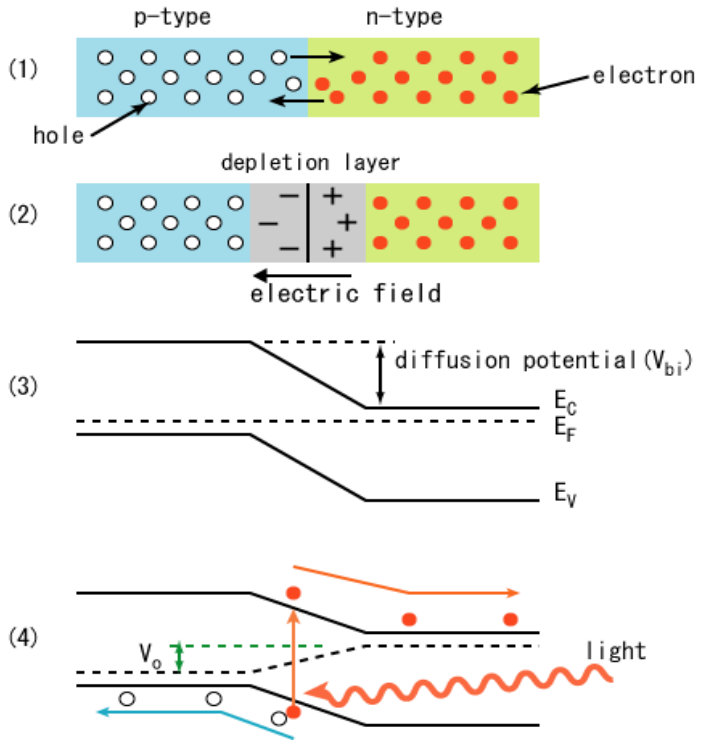

Figure 2.2: The p-n junction of an inorganic solar cell (open circuit); 1) electrons close to the junction, or boundary, diffuse into the p-type region; 2) charge builds up along the interface of the two materials, creating an electric field that opposes the flow of electrons; 4) a photon excites an electron into the conduction band, and the electron and its positive hole are forced to opposite ends of the cell by the intrinsic electric field.

2.2 Organic Photovoltaic cell:

The basic principle behind working of an organic solar cell is similar to that of the inorganic cell but a closer look reveals some significant differences in both the mechanisms. In inorganic theory, the incident light leads to instant generation of free charge carriers whereas, in an organic photovoltaic cell, absorption of photons leads to exciton generation. An exciton is a bound state of an electron and hole which are attracted to each other by the electrostatic Coulomb force.

Even the cell structures based on organic materials differ from that based on inorganic materials. Inorganic semiconductors generally have a high dielectric constant and a low exciton binding energy (eg. GaAs, BE= 4meV). Thus, at room temperature thermal energy being k_BT = 0.025eV, the excitons generated due to the absorption of a photon dissociate themselves into positive and negative charge carriers. Then, these free charge carriers are easily transported to their respective electrodes due to the already existing intrinsic junction

field and the high mobility of the charge carriers. On the other hand in organic materials the dielectric constant is much higher along with the exciton binding energies. The exact magnitudes of binding energies are still a mystery. For example poly-di-acetylene requires 0.5eV to split its exciton and thus dissociation of excitons cannot occur at room temperature. Exciton dissociation at the interface requires the offset between the bandgaps to be greater than the binding energy. To overcome the problem of high B.E., organic solar cells utilize two different materials that differ in the electron accepting and electron donating properties. Charges can then be created by photo induced electron transfer between the two (donor and acceptor) components of the photovoltaic device.

2.3 Elementary Processes in an Organic Solar Cell:

Working of an organic solar cell (OSC) can be primarily explained by four basic processes as follows:

1. Light absorption
2. Separation of the opposite charges (exciton formation)
3. Diffusion of excitons
4. Dissociation of Charge Carriers at the D/A Interface (Exciton dissociation)
5. Charge transport

2.3.1 Light absorption

Firstly, for efficient photon collection, the absorption spectrum of the active material in the organic solar cell should match the solar emission spectrum. Efficient overlap would lead to maximum absorption of photons hence maximum scope for photo excitation of electrons.

2.3.2 Exciton formation

Most solution processable semiconducting polymers have band gaps larger than 1.9eV, indicating that only 30% of the solar photon flux is covered. As, most polymers have low charge-carrier mobility, the thickness of the active layer is limited to about 100 nm, which in turn leads to the absorption of only about 60 % of the incident light at the absorption maximum (without considering the loss from the back reflection of the electrode) [31]. So, the organic materials with expanded absorption spectra up to 700-800 nm and high charge carrier mobility are favourable for efficient solar cells. As soon as the photon strikes an

electron, it gets excited from the donor`s HOMO to the donor`s LUMO creating a photoinduced charge (exciton) (Fig.2.3).

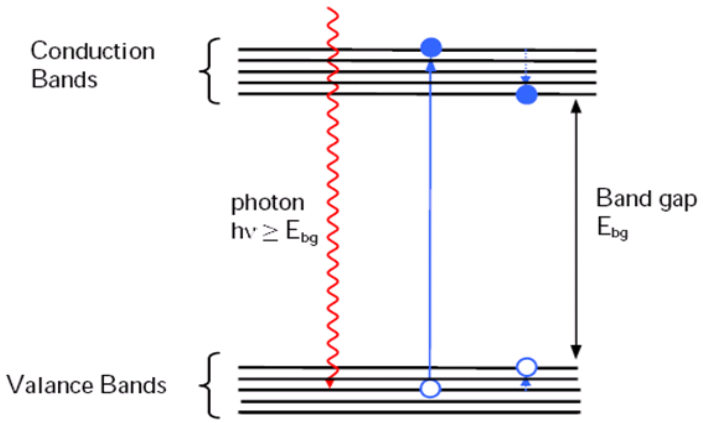

Figure 2.3: Charge separation due to the photon absorption

The missing electron in the valence band leaves a hole (of opposite electric charge) behind, to which the electron is attracted by the Coulomb force [32] leading to flow of charge.

2.3.3 Diffusion of Excitons

After the excitons are generated, they need to firstly dissociate to the donor/acceptor interface for the charge separation. Since the excitons dissociation process is confined to the D/A interfacial area, only excitons produced at a distance shorter than their diffusion length have the good possibility to reach the D/A interface where charge carriers are formed. Hence, for polymer-based solar cells, the exciton diffusion length L_D is an important parameter because the exciton diffusion process masters the photo-excitation energy transfer to the D/A interface. The exciton diffusion length L_D is defined as: $L_D = \sqrt{D\tau_0}$ where, D is the diffusion constant and τ_0 is the decay time constant. The exciton diffusion lengths in various conjugated polymers reported in the literature, differ very much, ranging from 5 to 20 nm [33, 34].

2.3.4 Dissociation of Charge Carriers at the Donor/Acceptor Interface

The electron is then transferred from an electron donor (D) a p-type semiconductor to an electron acceptor (A) an n-type semiconductor with the impact of photons (hυ):

D - A - hυ → D* - A (or D - A*) → D^- - A^-

Once the donor(D) and acceptor(A) gets excited, charge separated states consisting of the radical cation of the donor ($D^{-)}$ and the radical anion of the acceptor (A^{-}) are created. For efficient charge generation, the charge separated state should be the thermodynamically and kinetically most favourite pathway after photo-excitation.

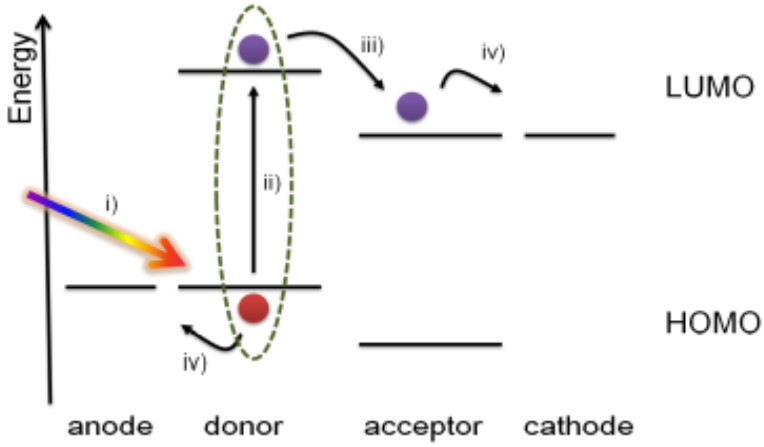

Figure 2.4*:* Simplified energy diagram showing the four elementary processes in an organic solar cell: i) light absorption, ii) exciton formation, iii) exciton dissociation at a donor acceptor interface and iv) charge extraction.

The electron in the donor moves from the highest occupied molecular orbital (HOMO) to the lowest unoccupied molecular orbital (LUMO) of the donor after the photo excitation as shown in Fig.2.4. Consecutively, the electron moves to the LUMO of the acceptor thus creating the charge separated states- $A^{\bullet-}$ and $D^{\bullet-}$. The charges thus formed are then collected at the opposite electrodes. On the other hand, similar process occurs when the acceptor is excited instead of the donor material. In a basic OSC, the donor and the acceptor materials are sandwiched between two dissimilar electrodes, one being a transparent electrode (ITO) and the other a metallic electrode for charge transport.

2.3.5 Charge Transport

After photo-induced electron transfer at the D/A interface and subsequent dissociation, the electrons are localized in the acceptor phase whereas the holes remain in the donor phase. Then, the free charge carriers must be transported via percolated pathways towards the electrodes to produce the photocurrent.

If donor and acceptor phases are perfectly 'bicontinuous' between the two electrodes, and all LUMO and HOMO orbitals are nicely matched, the carriers would be able to diffuse smoothly towards their respective electrodes (Fig.2.5). Except for the influence of phase separation and pathways properties, the instinct characteristics of charge carriers, i.e., charge carrier mobility μ, also plays a critical role in determining the fluency and efficiency of charge transport in the device.

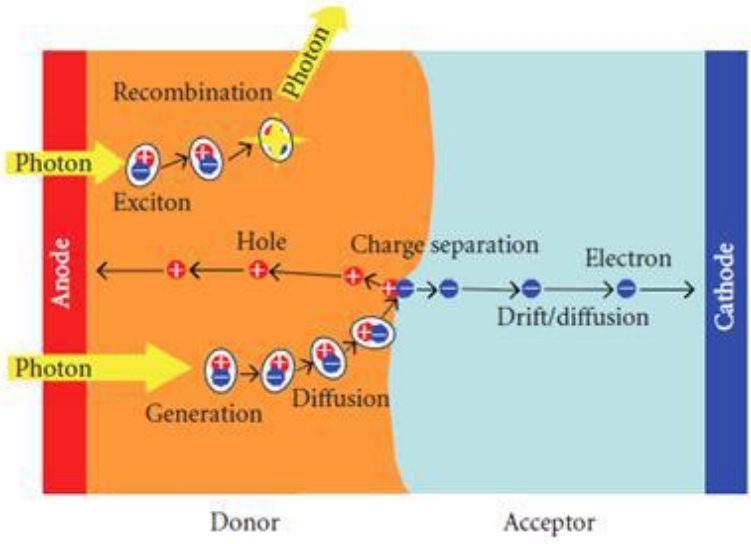

Figure 2.5: Principle of charge transport in a solar cell

The various existing structures of the OSCs had already been stated in the previous chapter. Among the various approaches to make organic solar cells, bulk heterojunction cells prove to be one amongst the best performing solar cells to due to the possibility of multiple interfaces and hence multiple junctions (between the p-type and n-type materials) in the cell. So, due to these advantages this thesis is majorly focussed on bulk heterojunction cells only.

2.4 Motivation

Interface layers have various functions in BHJ cells such as:

- They are able to reduce energy barrier between active layer and electrodes and can promote the formation of ohmic contacts for effective charge collection.
- They can form selective contacts for charge carriers.
- They can modify the electrode work function and can change conventional structure to inverted structure.

- They can protect active layer and can modify the field inside.

Interfacial layers in organic cells both in conventional as well as inverted structures play an important role in charge collection as well as for getting good device parameters and durability of devices. Mostly used interfacial layer is PEDOT:PSS. Other alternate materials are ZnO, TiO_x, V_2O_5, NiO and MoO_3 instead of PEDOT:PSS. However, major problems in using nanoparticles of the above mentioned oxides is the presence of defects during the film formation leading to poor electronic coupling with the active layer and rendering large series resistance.

Hence, alternative approaches are needed in view of creating low defect thin films of these oxides for proper coupling with the active layer. Herein we report a relatively new approach for using these oxides in organic solar cells for getting high efficiency as well as durability.

2.5 Characterization

Solar cells are characterised by measuring the current-voltage (I-V) curve under light illumination and dark. A typical current voltage (I-V) curve of a polymer solar cell is shown in Fig. 2.6. Since organic semiconductors show very low intrinsic carrier concentration, the metal-insulator-metal (MIM) model seems to be best suited to explain this characteristic. The characteristic points used to characterise a solar cell are labelled in Fig 2.6. In addition, for each of these points, the energy diagram for a single-layer cell with an indium tin oxide (ITO) anode and aluminium cathode is displayed. The point (a) on the curve corresponds to the current delivered by a solar cell under zero bias and is called short circuit current (I_{sc}). In this case, excitons dissociation and charge transport is driven by the so-called built-in potential. In the MIM picture, this potential is equal to the difference in work function (WF) of the hole and electron-collecting electrodes. For polymer solar cells, the transparent ITO (WF = 4.7eV) electrode is often chosen in combination with a low work function Al (WF = 4.24eV) [35] as counter-electrode to achieve a high internal field [36, 37]. Point (b) on the curve shows the voltage where the current equals zero is called open circuit voltage (Voc). In the MIM picture this situation is described by the case where the band is flat, since the applied voltage equals the difference in the work function of the electrodes. Point (c) on the curve is for V > Voc, the diode is biased in the forward direction. Electrons are now injected from the low work function electrode into the LUMO and holes from the high work function electrode into the HOMO of the organic layer, respectively. Point (d) on the curve is for V < 0, and the diode is driven under a reverse biased condition the solar cells works as a photodiode. The field is

higher than that at (a) which often leads to enhanced charge generation and/or collection efficiency.

An organic solar cell can be best characterized by carrying out its IV characteristics. This is done by measuring the current against different values of voltage across the cell. An ideal solar cell resembles a diode connected in parallel with a current source. In the absence of light, the I-V / J-V characteristics of the cell resemble that of a diode. On light absorption, charge is produced and hence current is generated in the device. The power generated is given by,

$$P = J\,V, \tag{1}$$

Where J being the current density and V is the voltage, maximum power generated can be calculated from the J-V curve. And the power conversion efficiency can be calculated using the relation,

$$e = \frac{Pmax}{Pin} \tag{2}$$

Fill factor (FF) is also an essential parameter in determining the solar cell performance. It is the ratio of maximum measured power to maximum theoretical power. Fill factor (FF) is given by

$$FF = \frac{J_{max}V_{max}}{J_{SC}V_{OC}} \tag{3}$$

Where, J_{SC} is the short circuit current density i.e. the current density when voltage equals zero and V_{OC} is the open circuit voltage i.e. the voltage when current equals zero.

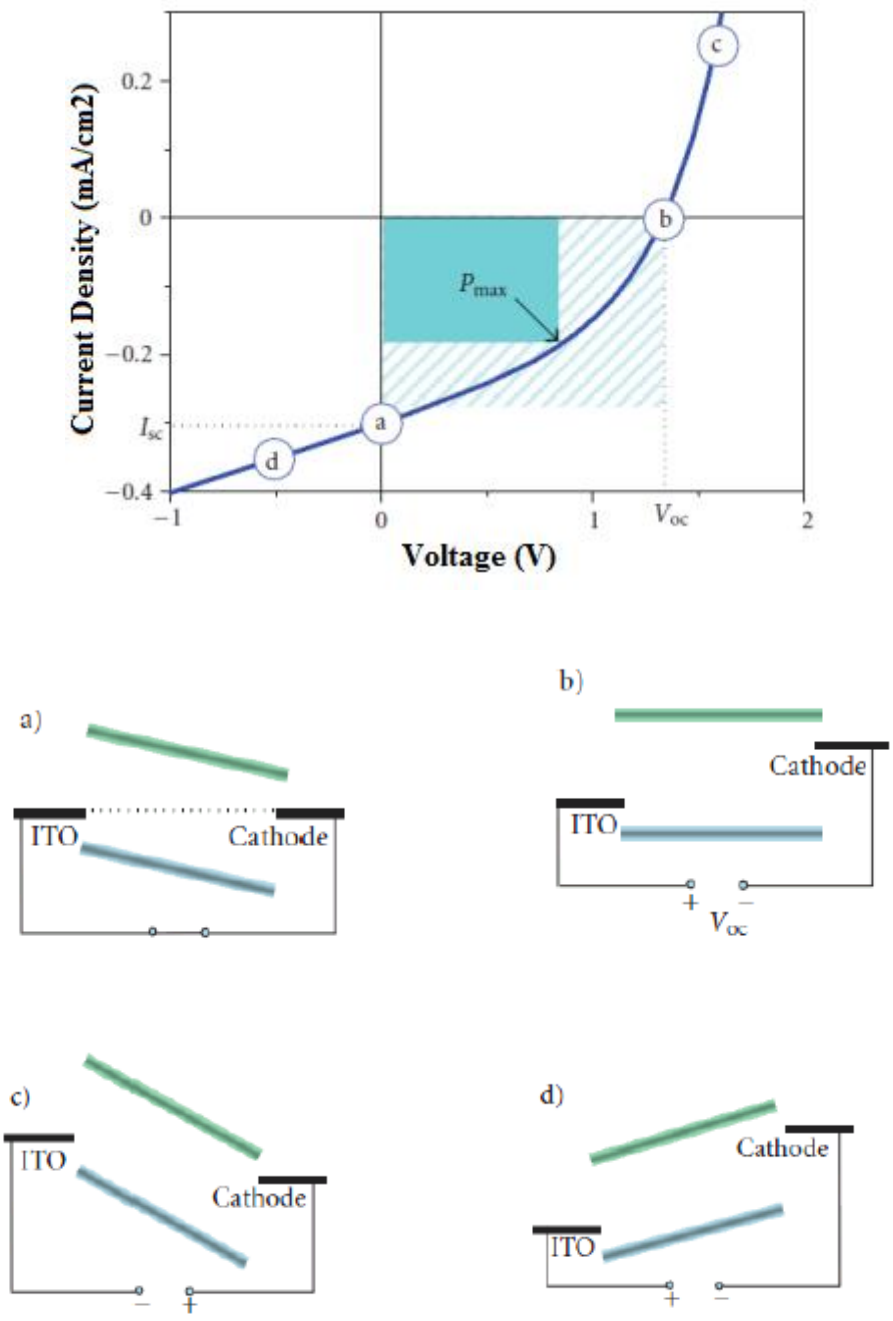

Figure 2.6: J-V characteristics of a typical organic diode shown together with the metal-insulator-metal (MIM) picture for the characteristic points. (a) Short circuit condition. (b) Open circuit condition. (c) Forward bias. (d) Reverse bias.

3. STRUCTURE, MATERIALS and TECHNIQUES USED

3.1 Structure

3.1.1 Geometry and construction

Organic solar cell has two basic structures so far as shown in Fig.3.1.

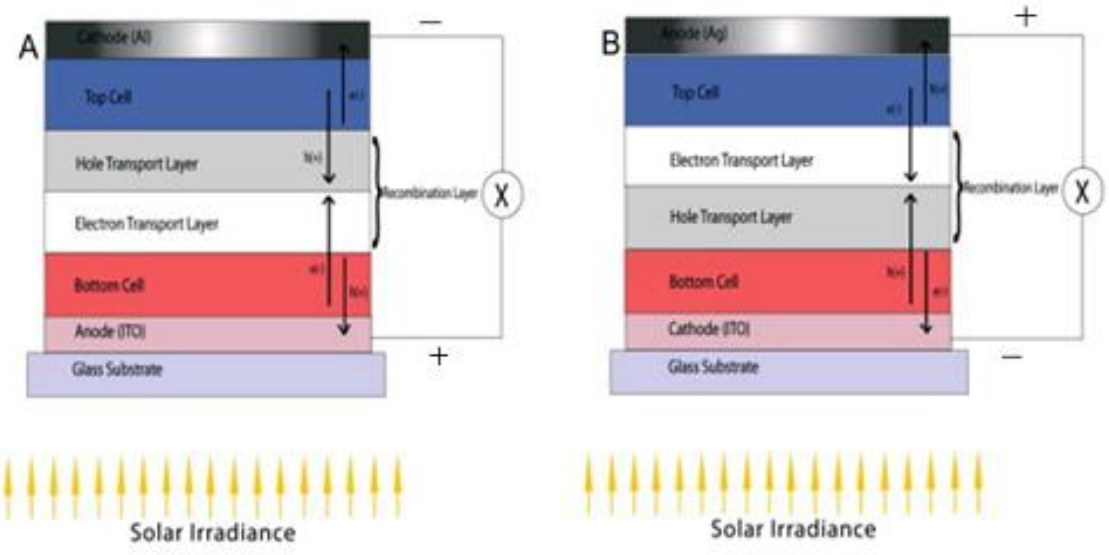

(a) (b)

Figure 3.1: Structure and geometry of bulk heterojunction solar cells.

a) Normal (Conventional) Cell. b) Inverted cell.

a) Conventional cell: In this, the transparent indium tin oxide (ITO) acts as an anode (for positive charge collection) and the metal electrode with lower work function as the cathode (for electron collection).
b) Inverted cell: As the name suggests, in this cell the electrodes are reversed. The ITO side is modified in a way that its work function falls below that of the metal electrode side and the electrons are then transported from the ITO, making it the cathode.

The two structures have advantages and limitations both. The conventional ones having high efficiencies have been recently challenged by the inverted generation due to their high stability and life time.

3.1.2 The Electrodes

An organic solar cell consists of two electrodes at the front and back of the cell. As mentioned earlier, in case of normal (or conventional) structure, the front electrode collects holes and the back electrode needs to have a higher work function. In case of inverted structure, the front electrode collects electrons. Here, the back electrode needs to have a lower work function compared to the front electrode.

The uppermost layer having direct contact with the solar radiation is of Indium Tin Oxide (ITO) which is a degenerated semiconductor comprising a mixture of In_2O_3 (90%) and SnO_2 (10%) with a band gap of 3.7eV and a Fermi level between 4.5 and 4.9eV with the desired etching over the transparent glass substrate. The choice of electrode materials largely depends on the work function of the material. It is the electrodes that collect the charges and facilitates charge separation and the relative work function decides the flow of opposite charges. As stated earlier, we use two electrodes in the solar cell-a hole collecting anode and an electron collecting cathode.

The work functions of ITO and grapheme are 4.8eV [38] and 4.5eV [39]. They have mid-range work functions and thus can serve as either anode or cathode. On the other hand, at the opposite extreme of the cell we should have an electrode that is usually a metallic and opaque. The metal electrode mostly Al that has a low work function (4.1eV [40]) and is generally used as the cathode.

The following are the requirements for a good choice of electrodes:

- A large difference in the work function of the electrode materials in order to achieve a large V_{OC}.
- The front electrode needs to be transparent in order to allow maximum light to reach the active layer and cause photo excitation of charge carriers.
- The back electrode is usually a metallic and opaque material.

So, in this project, keeping in mind the above mentioned requirements, we used metallic back electrode Al, processed via high-vacuum thermal evaporation as one of the electrode and the ITO coated glass as the opposite, depending on the cell geometry.

3.1.3 Intermediate/ Buffer Layers

The basic function of these layers is serving as either hole-conducting or electron-conducting materials. They are placed between active layer and the electrodes.

The main advantages of using an intermediate layer are:

- By allowing either positive or negative charge carriers to flow towards the corresponding electrode, it prevents recombination of the charges as it allows only single type of charge thus blocking the opposite ones. Certain thin interlayers such as Ca, CsF, or LiF(~1nm) film thermally evaporated on Al are known to provide better performance.
- Apart from these layers having a lower work function, they also act as a protective layer between aluminium and the active layer.
- It prevents the penetration of oxygen and water molecules into the active layer..

Based on the structure of the device we determine whether a hole conducting layer is required or an electron conducting layer. Different intermediate layers can be seen for conventional and inverted structures of organic solar cells in Fig. 3.1.

Another function is that, they may act as steps for electrons or holes in order to ease their path while moving from the active layer to the electrodes with mismatching energy levels. Also, these layers placed on top of the rough ITO, required for maximising photon scattering, prevent shunts and does not allow any alternative paths for current to pass [41]. The ITO is made rough for maximum photon scattering. It is well known that the electrical properties of intermediate layers are very important for the performance of the devices as they will affect charge transport at the interface. The conductivity of wide bandgap metal oxides (e.g., ZnO and TiO2) is sensitive to UV light [42-45].

The various buffer layers used in this thesis work are PEDOT:PSS and MoO_3 for conventional and ZnO, PFN, ZnO-PAS and ZnO-PVP for inverted geometry.

PEDOT:PSS or poly(3,4-ethylenedioxythiophene) poly(styrenesulfonate)

One of the most widely used intermediate layer is PEDOT:PSS or poly(3,4-ethylenedioxythiophene) poly(styrenesulfonate), a conjugated polymer, which is used as a hole conducting layer between the ITO and the active layer in a conventional cell [46]. Electron conducting layers include zinc or titanium oxide nanoparticles.

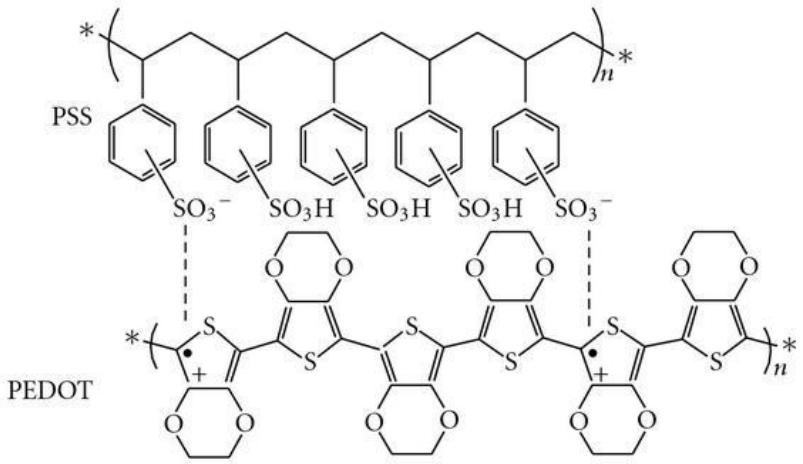

Figure 3.2: The chemical structure of poly(3,4-ethylenedioxythiophene) poly(styrenesulfonate) (PEDOT:PSS) [41]

Along with making the surface uniform, it also enhances the adhesion of the organic active layer onto the ITO (anode). The PEDOT:PSS film is semi-transparent with light blue colour. Its conductivity is comparable to that of metals [47]. Although, we still face some demerits of using PEDOT:PSS that is it's hygroscopic nature due to which water is introduced in the cell which later causes degradation in organic solar cell. For this reason there arises a new scope for the use of new materials as hole transport layer in conventional solar cells.

PFN or poly[(9,9-bis(3'-(N,N-dimethylamino)propyl)-2,7-fluorene)-alt-2,7-(9,9–dioctylfluorene) commonly.

PFN is a conjugated polyelectrolyte used as an electron-interface in OPV devices to improve extraction efficiencies. It is currently producing power conversion efficiencies of up to 9.2% [11]. And it is soluble in polar solvents such as water and methanol in the presence of small amounts of acetic acid.

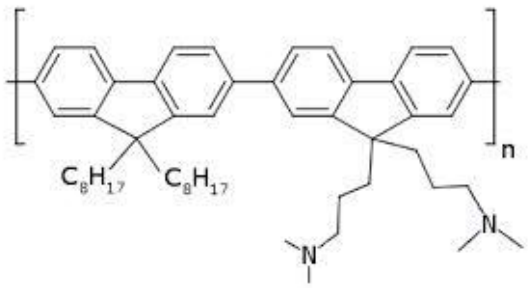

Figure 3.3: Chemical structure of PFN

PVP or Polyvinylpyrrolidone

It is also commonly called Polyvidone or Povidone, and is made from the monomer *N*-vinylpyrrolidone (Fig.3.4). PVP is soluble in water and other polar solvents. When dry it is a light flaky hygroscopic powder, readily absorbing up to 40% of its weight in atmospheric water. In solution, it has excellent wetting properties and readily forms films. This makes it good as a coating or an additive to coatings.

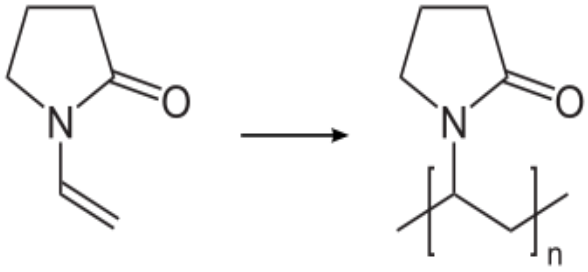

Figure 3.4: Chemical structure of PVP, made from the monomer *N*-vinylpyrrolidone.

PAS or Poly (acrylic acid sodium)

PAS is innoxious and soluble in water. It can be used in situations of alkaline and high concentration without scale sediment. PAS is used as scale inhibition and dispersant for circulating cool water system, papermaking, dyeing, ceramic, painting, etc. It is also named as Poly(Acrylate sodium); Polyacrylic Acid Sodium; Poly(acrylic acid sodium salt).

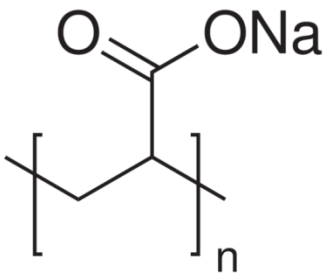

Figure 3.4: Chemical structure of PAS, Poly(acrylic acid sodium)

3.1.4 Active Layer

This layer is the origin of free charge carriers in the OSC. It consists of two materials i.e. acceptor and donor material that are spread in the entire bulk surface forming multiple p-n junctions. For preparing this solution, the two materials are mixed in desired proportions and left for stirring for atleast 24 hours. These materials should be mixed into a bi-continuous,

interpenetrating network (Fig.3.5) for the proper formation of junctions and pathways for exciton diffusion. This kind of bulk heterojunction was first explained by Yu et al. in 1995 [48].

Now, when the photons strike the active layer, which is basically the blend containing p-type and n-type material, charges called excitons are generated. The excitons then diffuse to the interface for charge separation where they are pulled towards their respective electrodes. The distance that the exciton travels before reaching the junction must be shorter than the exciton diffusion length for efficient charge separation otherwise the exciton loses its energy before reaching the interface and hence recombination occurs. Due to low mobility and short lifetime in case of single exciton diffusion, the diffusion length in organic semiconductors is about 8.0 ± 0.3 nm [40].

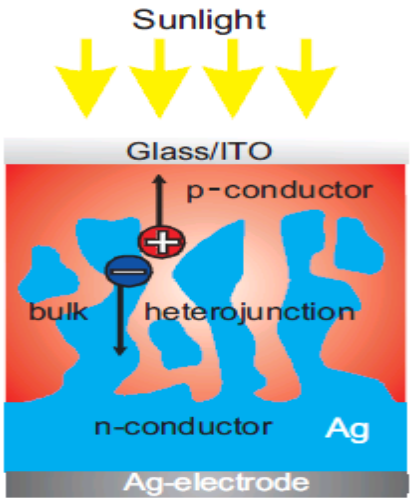

Figure 3.5: Diagram depicting the junctions present in the active layer.

The intrinsic tendency of the two materials- p-type and n-type, has lead to creation of phase separate on the nano-scale junctions (or interfaces) throughout the bulk of the layer.

For our investigation, we have used donor and acceptor combinations mentioned in literature viz; P3HT:$PC_{60}BM$ whose chemical structures are shown in Fig. 3.6. Main reason for this choice is its huge efficiency and good stability. P3HT (Poly(3-hexylthiophene-2,5-diyl)) is semi crystalline in solid state. It has a maximum absorption around 500 nm [49]. Due to its electron rich nature and high-energy HOMO level it's a good hole conductor. For a good acceptor, organic materials with high electron affinity are required. The acceptor material investigated in this thesis as acceptor is phenyl [6,6]- C61-butyric acid methyl ester ($PC_{60}BM$) - a soluble C-60 based compound (Fig 3.6(b)).

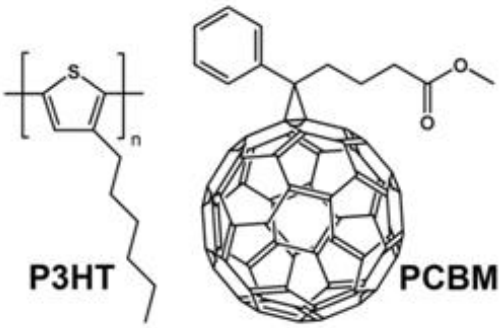

(a) (b)

Figure 3.6: Chemical structure of a) donor polymer P3HT b) acceptor PCBM

P3HT is based on thiophene units joined at the 2 and 5 positions in a head-to-tail geometry (Fig. 12(a)). To be able to dissolve the 'thiophene' a hexyl site group is added in the third position. PCBM forms crystalline domains in the bulk heterojunction with P3HT and it increases the hole mobility of the polymer. The reason for this is still being worked upon.

P3HT and PCBM is one of the most investigated combinations for the active layer and have large potential for high efficiency polymer solar cells. The active layer used in our present thesis work is a blend containing P3HT:$PC_{60}BM$, P3HT being donor polymer and PCBM being the acceptor.

All the materials used in this investigation were commercially bought from Sigma Aldrich.

The Table 3.1 below gives a list of the various materials that can be used as different interlayers and electrodes in various types of organic solar cells.

Table 3.1 Different materials used in conventional and inverted device structures

Cell Structure	**ETL**	**HTL**	**Anode**	**Cathode**
Conventional	Ca, CsF, LiF	PEDOT:PSS	ITO	Al, Ag, Au
Inverted	ZnO, TiO_2	MoO_3	Al, Ag, Au	ITO

3.2 Techniques Used

3.2.1 Standard Glove Box

It is a system that provides inert atmosphere for cell fabrication. There are two gloves for the user to insert his/her hands inside and perform tasks without affecting the seal. Most of the box being transparent enables the user to see and control what is being done inside. Two types of glove boxes exist: one allows a person to work with hazardous substances, such as radioactive materials or infectious disease agents; the other allows manipulation of substances that must be contained within a very high purity inert atmosphere, such as argon or nitrogen. It is also possible to use a glove box for manipulation of items in a vacuum chamber.

Figure 3.7: Glove box at NPL, New Delhi

For using the glove box, the initial step is to load the samples and apparatus inside via 'antechamber'. This is done in the following steps:

Transferring the materials into antechamber

- Refill the already evacuated antechamber and open its gate.

- Load the materials into the antechamber and then evacuate and refill it at least three times.

Transferring the materials from antechamber to glove box

- Make sure that both the refill valve and evacuation valve are closed.
- Insert hands & arms into the black rubber gloves with simultaneous lowering of the pressure inside using the left foot paddle.
- Open the inner lid of the chamber and move items in or out of the chamber.
- Check the door seal for any debris, and then swing the door back down and close it tight.
- Evacuate the antechamber at working time.

The glove box system is appropriate for carrying out different types of technique as spin coating, encapsulation, annealing etc. And even the thermal evaporation system is installed inside the glove box at NPL, New Delhi. After the completion the devices are taken out of the glove box again using the antechamber.

3.2.2 Spin Coating Technique

It is the most widely used deposition technique for the development of organic solar cells so far. Highly reproducible as well as very homogenous films can be deposited by this technique. Here, an excess amount of a solution is introduced on the substrate which is going to be accelerated to a chosen rotational speed in order to spread the fluid by centrifugal force, as shown in Fig. 3.8. The angular velocity of, substrate with the overlying solution gives rise to the ejection of most of the applied solution and only a thin film remains on the substrate. The key stages in spin coating are - deposition, spin-up, spin-off and evaporation [50].

The thickness, morphology and surface topography of the final film obtained from a particular material in a given solvent and at a given concentration is highly reproducible.

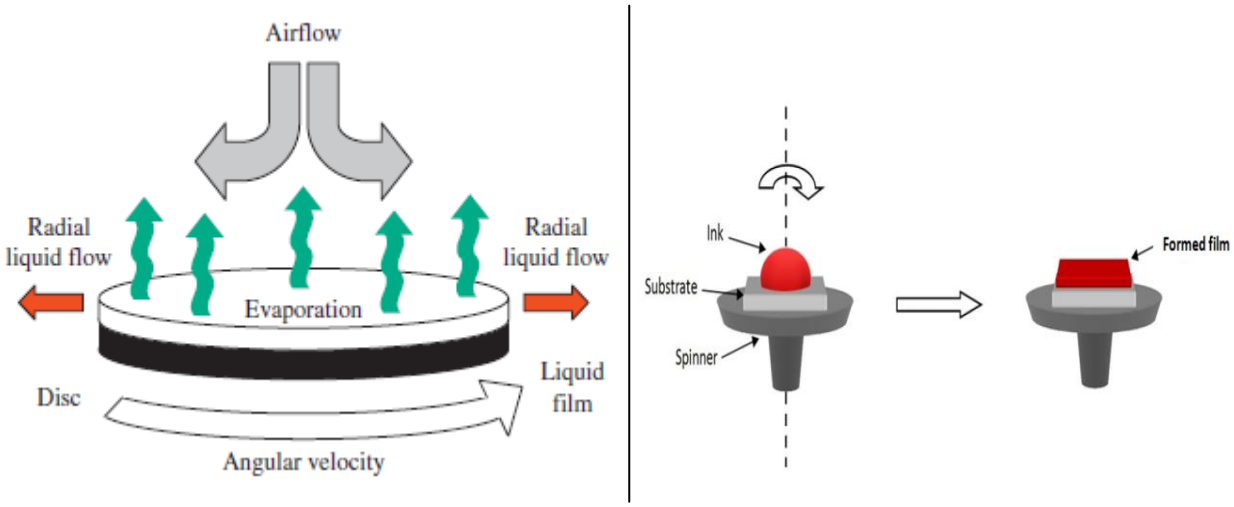

Figure 3.8: Schematic illustration of the spin coating technique

It has been commonly acknowledged that the spin coating technique is an excellent experimental technique on a laboratory scale. However, for commercialization of the OPV technology, where mass and large-scale production is required, spin coating lags behind.

Figure 3.9: Digital spin coater used at NPL, Delhi

3.2.3 Thermal Evaporation

Thermal evaporation is a widely used method to deposit metal films. The material to be deposited is kept on a boat. Here, electric resistance is used to heat the boat to extremely high temperatures. This causes the material kept on the boat to slowly melt and then evaporate onto the substrates kept above for deposition. The presence of ultra-high vacuum assures the formation of impurity free film on the substrate as impurities of the residual gas present in the working chamber are absent. Fig.3.10 gives the schematic diagram of thermal evaporation.

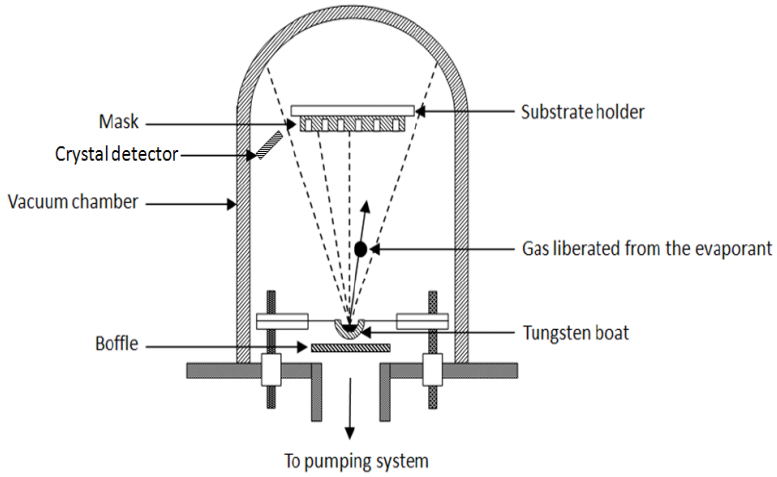

Figure 3.10: Thermal evaporator unit

The specifications of the system are mentioned below:

- Chamber pressure ~ 1 x 10^{-5} to 5 x 10^{-5} mbar.
- Typical filament current varies from 10 to 200 Amps.
- Tungsten or Molybdenum boats used to heat the evaporants.
- Maximum deposition thickness ~ 600 nm.

Vacuum is usually required to remove vapours other than the source material before the evaporation begins, because evaporated atoms may never reach the substrate if they collide with other foreign atoms too frequently, and furthermore, the collision may cause the evaporated material to react with foreign atoms. For instance, if aluminium is deposited in the presence of oxygen, it will form aluminium oxide instead of pure aluminium. So for aluminium deposition high vacuum is required (~10^{-5}-10^{-6} mbar). The various pumps used for creating the vacuum are described below.

Vacuum Technology

The different pump technologies used in thermal evaporation technique are: rotary pump and turbo pump.

a) **Rotary Vane Pump:**

The rotary pump is an oil sealed rotary displacement pump. See Fig. 3.11. It essentially consists of: Pump housing, an eccentrically installed Rotor, Vanes and a Spring.

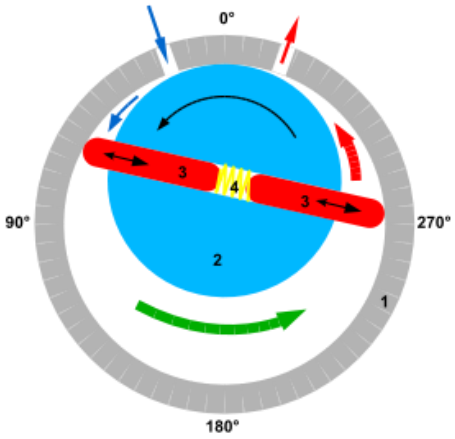

Figure 3.11: A rotary vane pump with its various parts as: 1. Pump housing, 2. Rotor, 3. Vanes, 4. Spring.

The simplest vane pump is a circular rotor rotating inside of a larger circular cavity. The centres of these two circles are offset, causing eccentricity which enables them to slide into and out of the rotor and seal on all edges, creating vane chambers that do the pumping work. The inlet is attached to the space with increasing volume and the outlet is attached to the space with decreasing volume. As the volume of the space increases, a low pressure is generated within the space i.e. vacuum forcing air to flow in from the inlet. Whereas, when the volume in the second space within the working chamber decreases, a high pressure is generated within thus causing the air to be discharged from the outlet connected. The action of the vane drives out the same volume of fluid with each rotation. Multistage rotary vane vacuum pumps can attain pressures as low as 10^{-3} mbar (0.1 Pa).

b) **Turbomolecular Pump:**

These pumps are used in ultra-high vacuum (UHV) systems. The mechanism used in this pump is imparting momentum to the molecules in a particular direction by repeated collision with a solid surface.

As the gas molecules enter through the inlet, the rotor, with a number of angled blades, hits the molecules. Thus the mechanical energy of the blades is transferred to the gas molecules. With this newly acquired momentum, the gas molecules enter into the gaps in the stator. This leads them to the next stage where they again collide with the rotor surface, and this process is continued, finally leading them outward through the exhaust. Because of the relative motion of rotor and stator, molecules preferentially hit the lower side of the blades.

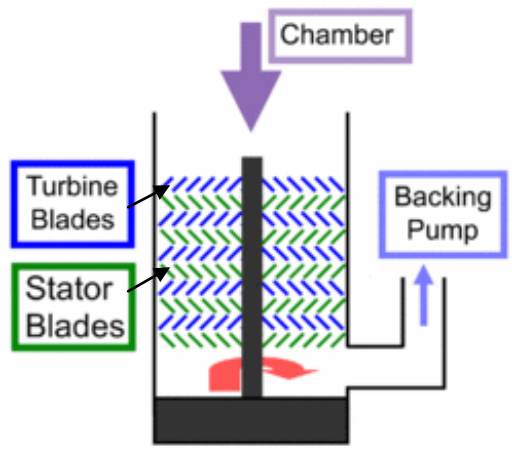

Figure 3.12: Lateral view of a turbomolecular pump

Fig. 3.12 shows the lateral view of the inside of a turbomolecular pump. It consists of stack of rotor disks. In between rotor disks are stators. Gas captured by the upper stages is pushed into the lower stages and successively compressed to the level of the fore-vacuum (backing pump) pressure. So, this pump always need a backing pump along with it, that is also responsible for roughing of the chamber before turbo could function.

The turbomolecular pump can be a very versatile pump. It can generate many degrees of vacuum from intermediate vacuum (~10^{-2} Pa) up to ultra-high vacuum levels (~10^{-8} Pa).

4. ORGANIC SOLAR CELL FABRICATION

4.1 Active Layer Preparation

Before we start anything, it is recommended to prepare the active layer as for best results it requires atleast 24 hours stirring. For this, the polymers P3HT and $PC_{60}BM$ were taken in desired concentrations. In the current thesis work we used 3:2 ratio of P3HT:$PC_{60}BM$ i.e. 18mg (P3HT) and 12mg (PCBM) in 1 ml chlorobenzene solution. The materials were put in properly cleaned vials along with a magnetic bead. The blend was then kept on stirring overnight to make the best possible blend of the two.

4.2 Etching of the ITO sheet

Firstly, the ITO glass sheet was cut into 3 x 3 inch square substrates using a diamond cutter. These substrates were then undergone laser etching, where the ITO region over the glass was etched/removed in such a way that it left two parallel strips, each of 0.2 cm thickness of ITO. In this pattern, once the fabrication was complete, we got four independent pixels due to perpendicular deposition of the metal electrode.

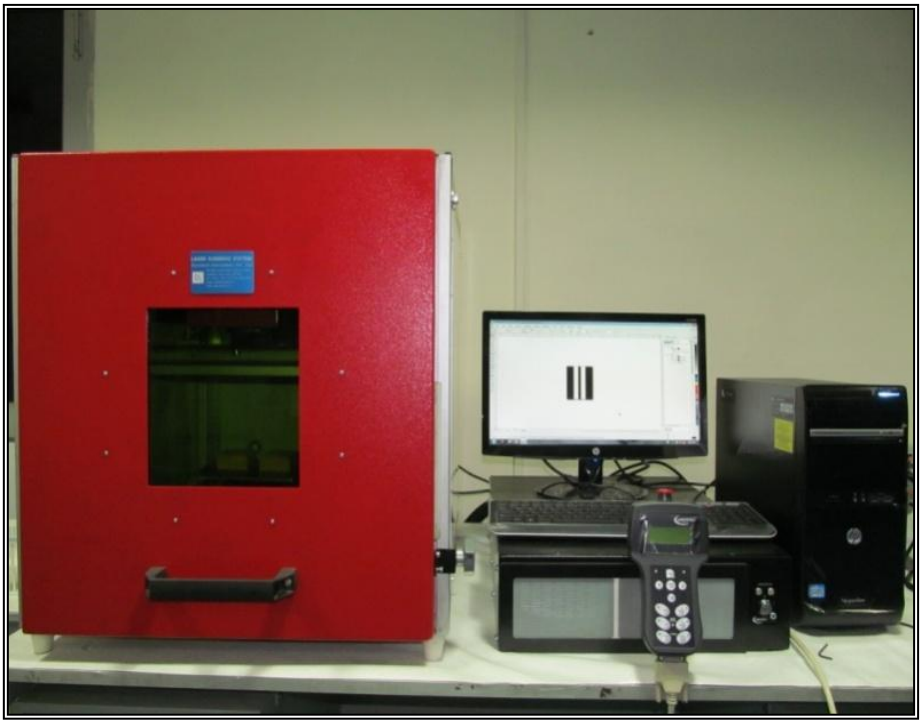

Figure 4.1: Laser Scribing Unit at NPL, Delhi

4.3 Cleaning of the ITO glass slide

4.3.1 Soap Treatment

Cleaning is a primary as well as an important step in the cell fabrication because even a single particle or stain can disturb the uniformity of the film. The patterned ITO substrates were wiped with acetone to remove the dust and then, sonicated for 20-30 minutes in soap water. Ultrasonic cleaning is a process where ultrasonic sound is used to energise the liquid molecules, usually water, which forcefully removes all the particulate impurities adhered to the surface of the substrates [51].

Then the substrates were rubbed by the liquid soap using cotton multiple times until we could see a thin layer of water rest at the surface for a few seconds before falling down (Fig. 4.2(a)). This step removes all the oil contaminants. After this, the cleaned samples were kept in distilled water for ultrasonication to ensure removal of all organic solvents from the sample surface (Fig. 4.2(b)).

(a) **(b)**

Figure 4.2: Cleaning of the ITO substrates

(a) Soap cleaning of the substrate (b) Ultrasonic treatment of the substrates

4.3.2 Boiling in various solvents

After the soap treatment, the samples are boiled in three different solvents.

- Firstly, in acetone for around 15-20 minutes in order to remove all the water droplets from the substrates.

- Then, in trichloroethylene (TCE) for another 20 minutes. The substrates were dried in the solvent fumes every time they were transferred from one solvent to another. While boiling in TCE, if any impurities were still observed, they were manually removed using cotton wrapped over a pair of foreceps. This step removes all the acetone from the substrate surfaces.
- Finally, the samples were made to boil in isopropanol (ISP) for another 15-20 minutes to removing all the TCE traces.
- The dried (in ISP fumes) substrates were kept in a clean and dried petridish and were kept for proper drying in an oven at around 150°C for 30 minutes.

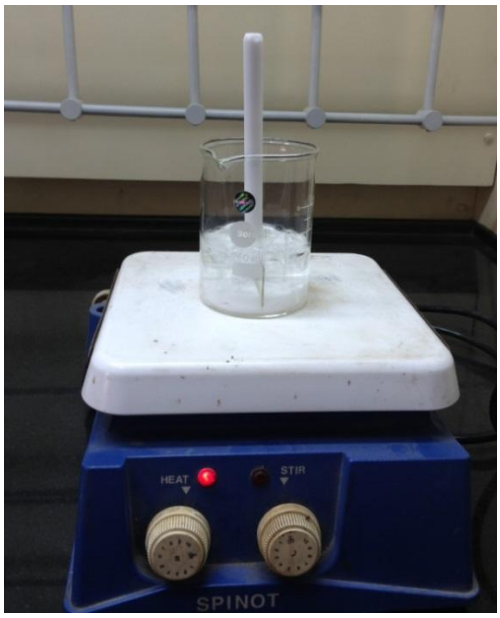

Figure 4.3: Boiling of the ITO substrates

4.4 UV Ozone Treatment

The morphology of the ITO surface and the oxygen defects are known to be important factors in determining the charge injection at the interface [52]. Treatments such as chemical treatment (aquaregia, RCA), and plasma treatment, and UV-ozone treatment can increase the ITO work function, which may be due to surface carbon removal, creation of surface dipoles, a change in the ratio of surface constituents (Sn, In, O). After the complete cleaning, the etched ITO substrates are exposed to UV ozone gas. Prior to grafting of the polymers onto the substrates, they were treated with UV/ozone to activate their surfaces. To optimize the UV/ozone treatment time, contact angle was measured over a time period with the duration of

UV/ozone treatment from 0 to 30 min. The contact angle of the treated substrates decreased greatly with UV/ozone treatment. This means that the polymers stuck to the surface much better post the UV ozone treatment than they did without that. A 20 minute UV ozone exposure was found enough to modify the ITO surface favourably in order to enhance the buffer/polymer holding capacity.

4.5 Buffer Layer Solutions Preparation

The buffer layers solutions were synthesized using solution route. The following buffer layers were used for the present investigation

For conventional device-:

- PEDOT:PSS
- MoO_3 solution

For inverted device-

- ZnO solution
- ZnO-PAS nanocomposite
- ZnO-PVP solution
- PFN solution

MoO_3 Solution

For this, 0.4 g of ammonium heptamolybdate salt was dissolved in 10 ml of distilled water. This solution was stirred and heated at 80º C for 1 hour. Now different weight percentages of this solution were made. For instance: for 1 wt. %, 1 g of this solution was added in 99 g water and so on. Now different weight percents (0.2 – 2) were used as buffer layer in the experiment conducted.

ZnO Solution

0.235 g of zinc acetate dihydrate was added in 5 ml propanol and allowed to stir for 5 min. A white cloudy solution is obtained here. Now after 5 minutes, few drops of diethanolamine (DEA) are added to this solution. DEA acts as a stabilizer. Slowly we will observe that the cloudiness disappears and a colourless and transparent solution is obtained. Now, this

solution is stirred at 60°C for 2 hours. The solution is then kept untouched and undisturbed for 24 hours. After coating this solution on ITO, the substrate is heated at 200°C for 30 minutes.

ZnO-PAS nanocomposite solution

To make PAS solution we added 0.5 ml PAS in 0.5 ml of water. This solution was stirred for 30 minutes. Now to prepare the nanocomposite solution, this 1 ml PAS solution was added in 2 ml of ZnO solution. Also after a 5 minute interval, 2 to 3 drops of DEA were added in this solution and the resultant mixture was then stirred for 30 minutes.

ZnO-PVP solution

Firstly 2.5mg PVP was dissolved in 1ml water. And 11mg zinc acetate dehydrate was dissolved in 1ml water separately. Both the solutions were mixed and 5ml ethanol was added to the mixture. The final solution was treated with few drops of diethanalomine (stabilizer) and kept on stirring for 30 minutes.

PFN solution

8 mg of the Polymer poly [(9,9-bis(3'-(N,N-dimethylamino)propyl)-2,7-fluorene)-alt-2,7-(9,9–dioctylfluorene) commonly known as PFN was taken. Then it is mixed in the solution of 4ml of methanol and 10µl acetic acid. The solution was kept for magnetic stirring for atleast 48 hours. The final solution was filtered using a pvdf hydrophyllic filter before use.

4.6 Buffer Layer Coating

The ozone treated samples are made ready for the buffer layer coating. For the conventional cells, according to the sequence, this position is occupied by the PEDOT:PSS layer or other alternatives depending on the cell geometry as in Table 1. The ITO substrate is kept inside the spin coating device, held by very high vacuum. Care must be taken while placing the substrate with its ITO side facing upwards. The device is set to the desired rpm (rotations per minute) for the required time as shown in Table 4.1.

Table 4.1: Table showing the optimized rotation speeds and time used in the experiments conducted.

S.NO.	Buffer layer	Rpm	Time (seconds)
1.	PEDOT:PSS	2000	60
2.	MoO_3	4000	30
3.	ZnO	2000	60
4.	ZnO-PAS	3500	60
5.	ZnO-PVP	2000	60
6.	PFN	5000	60

After the threshold vacuum is attained, the solution to be coated is put over the ITO side using a micro pipette, enough to cover its entire surface. Finally the device runs for the pre-set time giving a fine and uniform layer for further processes.

4.7 Buffer Layer Annealing

The samples were then kept for annealing in air or in vacuum as per the demand of the cell structure at desired temperature as shown in the Table 2 below.

Table 4.2: The required annealing temperatures for various buffer layers

S.NO.	Buffer layer	Temperature (^oC)	Time (minutes)
1.	PEDOT:PSS	120	20
2.	MoO_3	100	10
3.	ZnO	200	30
4.	ZnO-PAS	200	30
5.	ZnO-PVP	200	30
6.	PFN	No annealing	-

Here, 1 and 2 layers correspond to conventional cell and 3, 4 and 5 to inverted cell geometry.

4.8 Active Layer Coating

After the desired annealing, the samples are ready to be spin coated by the active layer that had been prepared in advance as described in section 4.1. It is preferred to filter the active layer using a syringe and a PVDF filter in order to avoid any non-uniformity in the film due

to undissolved blend material. The filtered P3HT:PCBM blend was then spin coated over the substrates at 1000 rpm for 1 minute.

4.9 Active Layer Annealing

The substrates were kept for vacuum annealing at 120º C for 20 minutes in vacuum oven. This process should not be carried out in air as oxygen diffuses into the active layer and degrades the material. The changes in surface morphology due to thermal annealing have been noted in the results section. Once annealing is complete next is the thermal evaporation step.

4.10 Thermal Evaporation

In both conventional as well as inverted cells, aluminium is deposited by thermal evaporation. The only additional step required in case of inverted cells is the deposition of MoO_3 just before aluminium. As described in section 3.2.4, this process involves the current heating of a filament (or boat) in a vacuum chamber. Ultra high vacuum (UHV) is needed for this process. Before the evaporation starts, the filament used for keeping the metal to be deposited, needs to be flashed in order to remove the impurities. For this too, one needs a high vacuum and high temperature to burn off the impurities stuck on the tungsten filament used.

Figure 4.4: Thermal Evaporation Unit at NPL, New Delhi

Pressure up to 9 x 10^{-6} mbar was attained in the chamber. The process specifications used are:

- MoO_3 deposition: (For inverted cells)
    - Power- 30 W
    - Deposition Rate- 0.5 A°/sec
    - Thickness-7.5-8 nm
- Aluminium deposition: (For both-inverted as well as conventional devices)
    - Power-35 W
    - Deposition Rate- 5 A°/sec
    - Thickness-125 nm

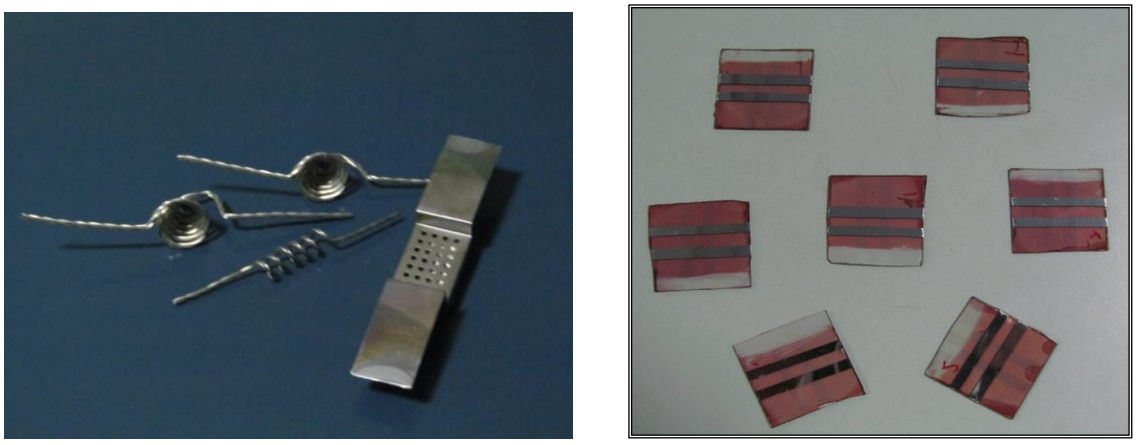

(a) **(b)**

Figure 4.5: (a) Filaments used in thermal deposition process; (b) Organic Solar Cells Fabricated

Once deposition is complete, air is slowly passed into the chamber. The rate is maintained low so as to avoid any major dust particles from entering the chamber and settling on the substrate.

4.11 J-V Characterization of the Device

After the complete fabrication, the J-V characteristic are taken in open atmosphere and recorded by the Keithley SourceMeter unit. A tungsten halogen lamp from Osram, Germany, was used to illuminate the cells at intensity 100mW/cm^2 (Fig.4.7). For measurement of J-V characteristics the applied voltage was swept from -0.5V to -1V in the step of 0.02 V and the

corresponding current was measured and recorded using Keithley 2420 SourceMeter unit interfaced with computer. The measurements were done both in illuminated and dark conditions.

Depending on the structure of the device, the positive and negative terminals of the Keithley unit are attached with the anode and cathode terminals of the device respectively. Using the current and voltage characteristics fill factor (FF), open circuit voltage (V_{OC}), and power conversion efficiency (η) were measured.

Figure 4.6: Set-up for J-V characterization of the device.

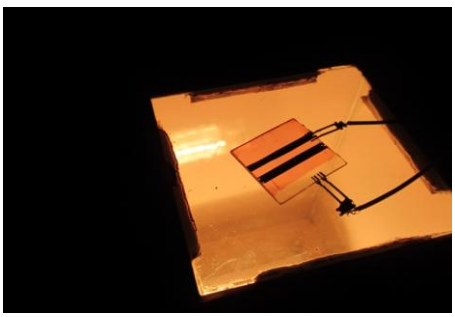

Figure 4.7: A device being illuminated for J-V characteristics

5. Results and Discussion

5.1 Conventional Devices

We have known this as a fact that conventional devices show inferior stability as compared to inverted devices. In our thesis work we started with the conventional structure and approached towards the inverted one. We started with the fabrication of device using PEDOT:PSS as the hole transport layer (HTL) and the device structure (Fig.5.1) used is:

ITO|Buffer Layer|P3HT:$PC_{60}BM$|Al

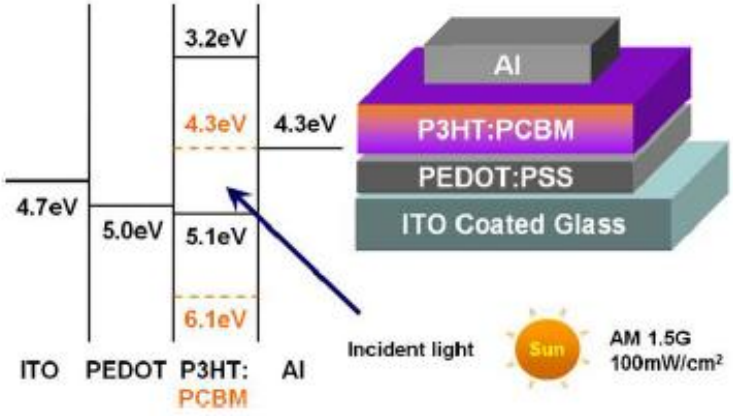

Figure 5.1: The energy diagram for ITO/PEDOT:PSS/P3HT:PCBM/Al cell.

5.1.1 Organic solar cell devices based on PEDOT:PSS as the hole transport layer (HTL)

PEDOT:PSS was coated on the cleaned ITO substrate at different rotation speeds of spin coater. The obtained J-V characteristics for various rotation speed of the spin coater have been plotted in Fig. 5.2 and the device parameters are presented in Table 5.1

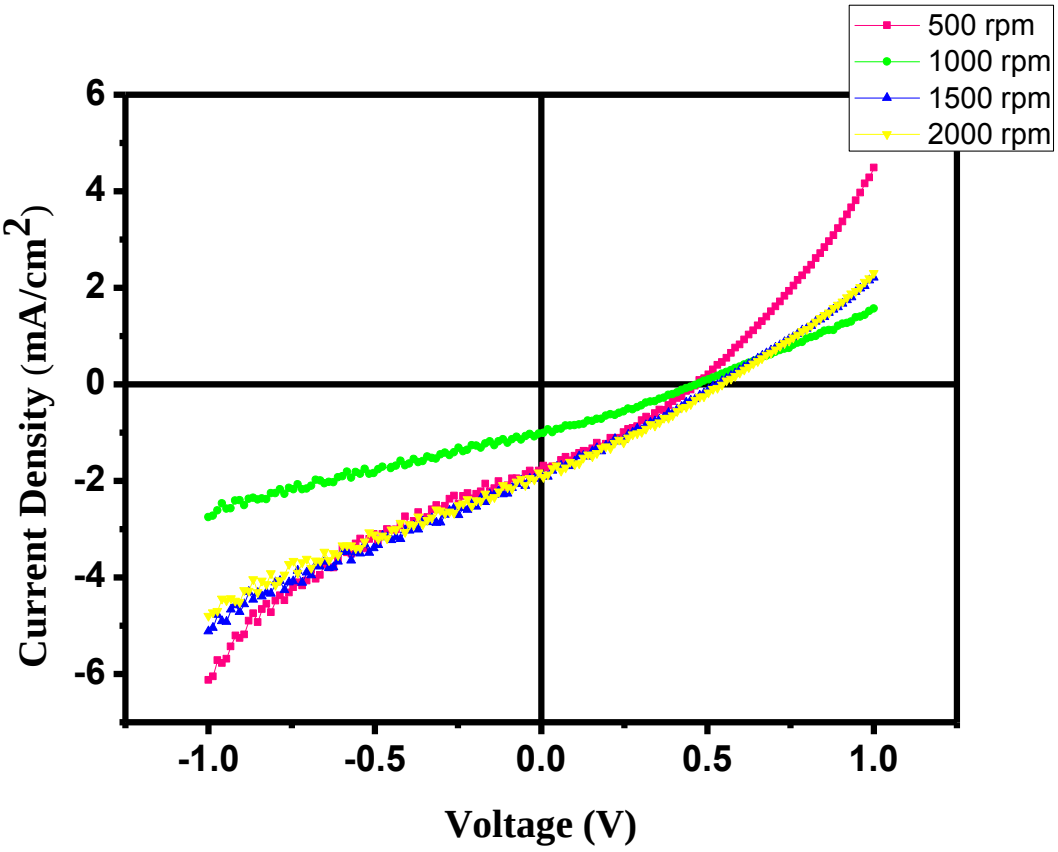

Figure 5.2: J-V plot at different thickness levels of PEDOT:PSS in solar cell with device structure ITO|PEDOT:PSS|P3HT:PCBM|Al

Table 5.1 Device Parameters of ITO|PEDOT:PSS|P3HT:PCBM|Al

Rotation Speed	Fill factor (FF)	V_{OC} (V)	J_{SC} (mA/cm^2)	PCE (%)
500 rpm	32.3	0.476	1.69	0.26
1000 rpm	29.6	0.477	1.01	0.142
1500 rpm	27.7	0.544	1.91	0.286
2000 rpm	27.9	0.557	1.92	0.3

It was observed that the change of rotation speed of spin coater does not make any difference in the overall device performance. It is obvious from Fig. 5.2 that the device suffers serious problem of leakage current. The series resistance of the device is also high hence; we are

unable to obtain good shape of the J-V curve. The device parameters (Table 5.1) remain near constant irrespective of the change of rotation speed.

Further, PEDOT:PSS is hygroscopic, acidic, corrosive and its properties such as conductivity changes with change of manufacturer. Hence, we started looking for the replacement of PEDOT:PSS with alternative materials such as- MoO_3, NiO and V_2O_5.

Now we know that engineering of interfacial carrier transport layers between organic layer and metallic electrodes is one of the major aspects in designing OSCs. Among various materials available for interfacial layers, transition metal oxides have great potentials owing to the following:

- Wide range of energy level aligning capabilities
- Formation of low resistance ohmic contact by these oxides
- High transparency and desirable band structure
- Excellent ambient stability in ambient environment which can extend the lifetime of organic electronics

The above factors, energy level compatibility (visible in Fig. 5.3), low cost and high throughout production using solution route makes MoO_3 as the most attractive alternative to PEDOT:PSS.

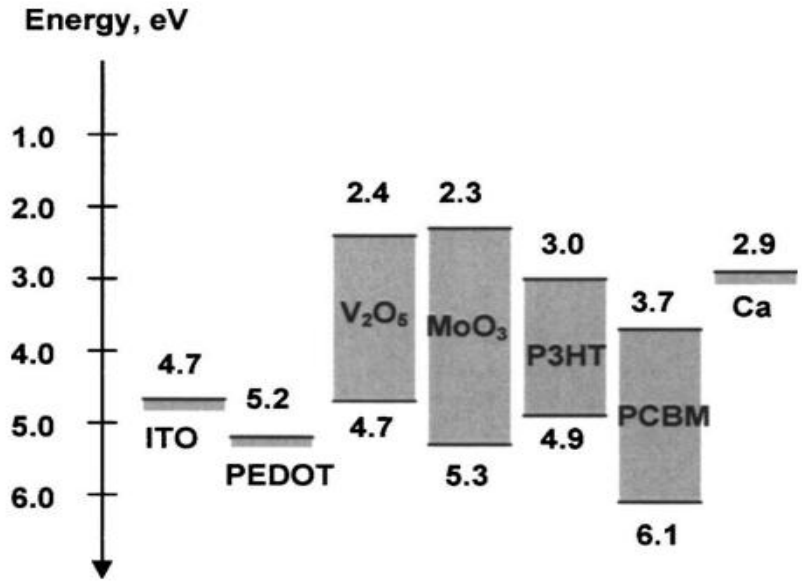

Figure 5.3 Schematic comparing the energy levels of various layers used in OPVs [53]

5.1.2 Replacing PEDOT:PSS with MoO_3

The MoO_3 is synthesized through solution route. Figure 5.4, 5.5 show the devices using solution processed MoO_3 as an interface layer in OSC. The concentration of the MoO_3 solution used in Fig.5.4 is 2 wt%. Using this MoO_3 HTL the solar cell showed a fill factor (FF) of 32.8%. The V_{OC} and J_{SC} values were 0.51V and 0.71mA/cm^2 respectively. The power conversion efficiency (PCE) value obtained is 0.12%.

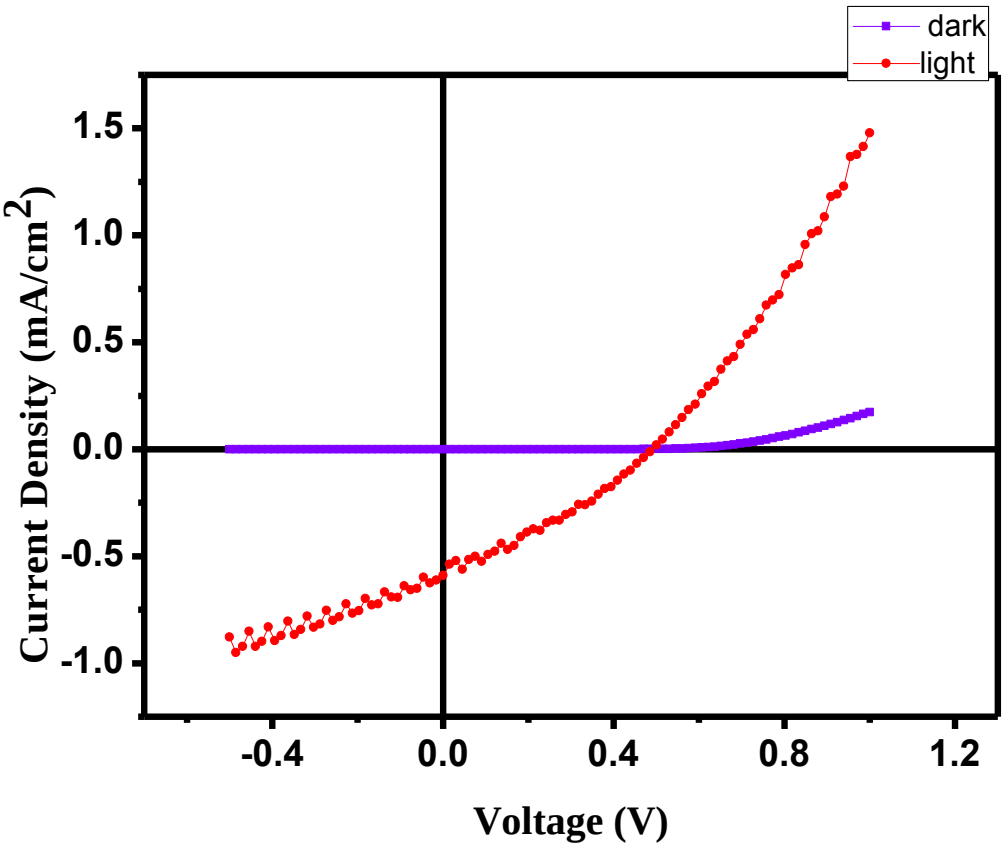

Figure 5.4: J-V plot for solar cell with device structure ITO|MoO_3|P3HT:PCBM|Al

It is clear from the J-V plot that the shunt resistance in the device is negligible due to the near ideal dark characteristics obtained. There is some leakage present in the device too. When MoO_3 is spin coated, MoO_3 nanoparticles may agglomerate and may not give uniform surface morphology. This may increase the roughness of the film which may lead to leakage current

Optimization of MoO_3 film concentration

In view to see the effect of MoO_3 layer thickness on device performance we have tried different concentration of MoO_3 solution (0.2 -2 wt %). The J-V plot in light has been shown in Fig. 5.5.

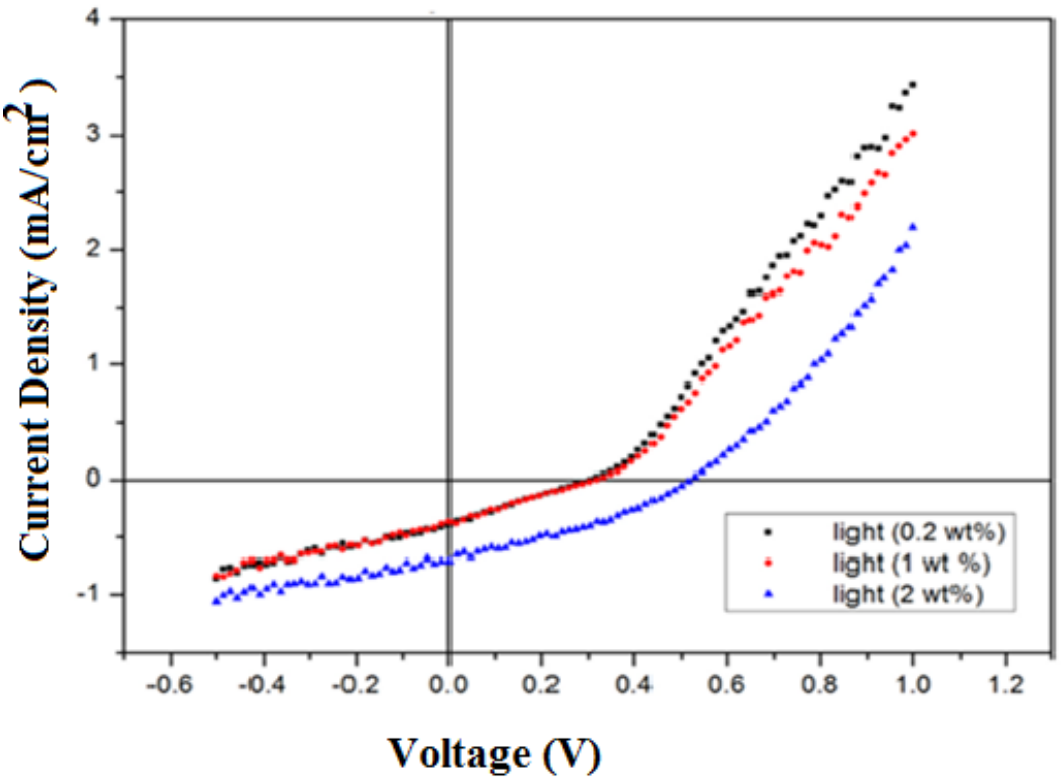

Figure 5.5: J-V plot in light condition for varying concentration of MoO_3 in solar cell with device structure ITO|MoO_3|P3HT:PCBM|Al

Table 5.2 Device parameters of ITO|MoO_3|P3HT:PCBM|Al

Concentration (Wt. %)	Fill factor (FF)	V_{OC} (V)	J_{SC} (mA/cm^2)	PCE (%)
0.2	23.6	0.30	0.419	0.0030
1	24.6	0.30	0.391	0.0029
2	32.8	0.51	0.71	0.120

It is obvious from Table 5.2 the device ITO|MoO_3|P3HT:PCBM|Al has given the best device parameters for the concentration of 2wt% of MoO_3. As we lower the concentration of MoO_3, the performance of the solar cell decreases. However, still more studies such as AFM, EDAX are needed to confirm which concentration of MoO_3 gives better film as well as better device performance.

Thus, MoO_3 has the potential to be a good replacement for PEDOT:PSS. Further optimization of the film is required to obtain better device and device efficiency.

Although conventional devices display good performance, these devices degrade at highrer rates in air. Extensive investigation of polymer solar cells with an inverted device structure, using modified ITO as cathode is required. These inverted devices are felt to be better as these do not use corrosive PEDOT:PSS and low work function metal cathodes. Further, inverted devices have an advantage of vertical phase separation and concentration gradient in the active layer which shows the self-encapsulating property as air stable materials are used as top electrode. Hence, we have chosen these ideal devices for our study.

5.2 Study of Inverted Device

For our investigation we chose the following device structure:

5.2.1 Using ZnO as Electron transport layer (ETL)

ITO|ZnO|P3HT:PCBM|MoO3|Al

ZnO is good choice because of its environmental stability, relatively high electron mobility and optical transmittance [54] and its wide and direct bandgap (3.37 eV) (Fig. 5.6).

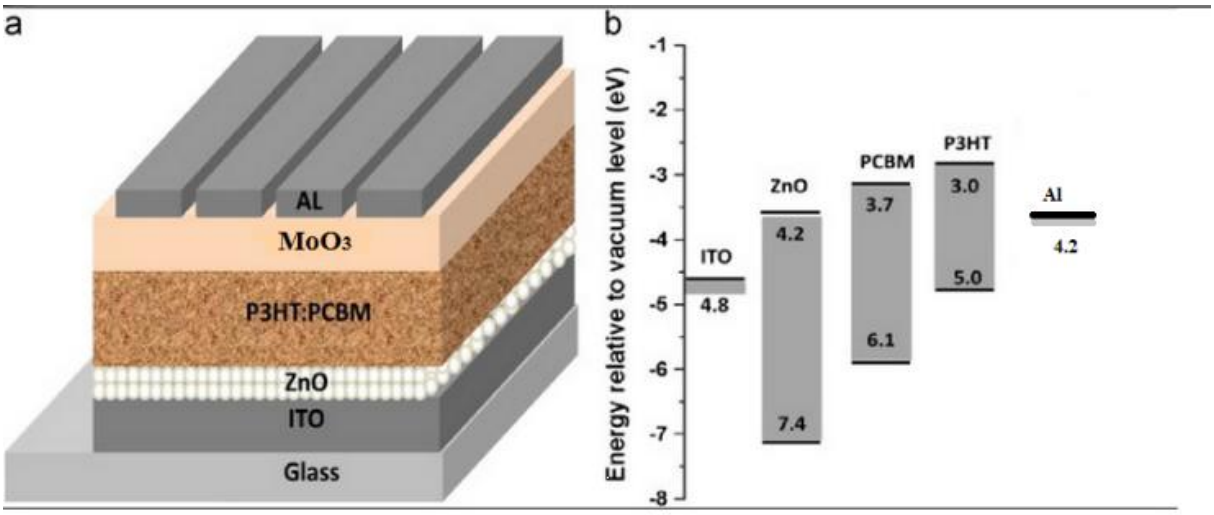

Figure 5.6: Energy level diagram of ZnO relative to other layers of the inverted structure.

ZnO film prepared by solution process as explained in section 4.5. After coating this solution on ITO at 2000 rpm, the substrate was heated at 200°C for 30 minutes. The active layer tried out with ZnO was P3HT:$PC_{60}BM$.

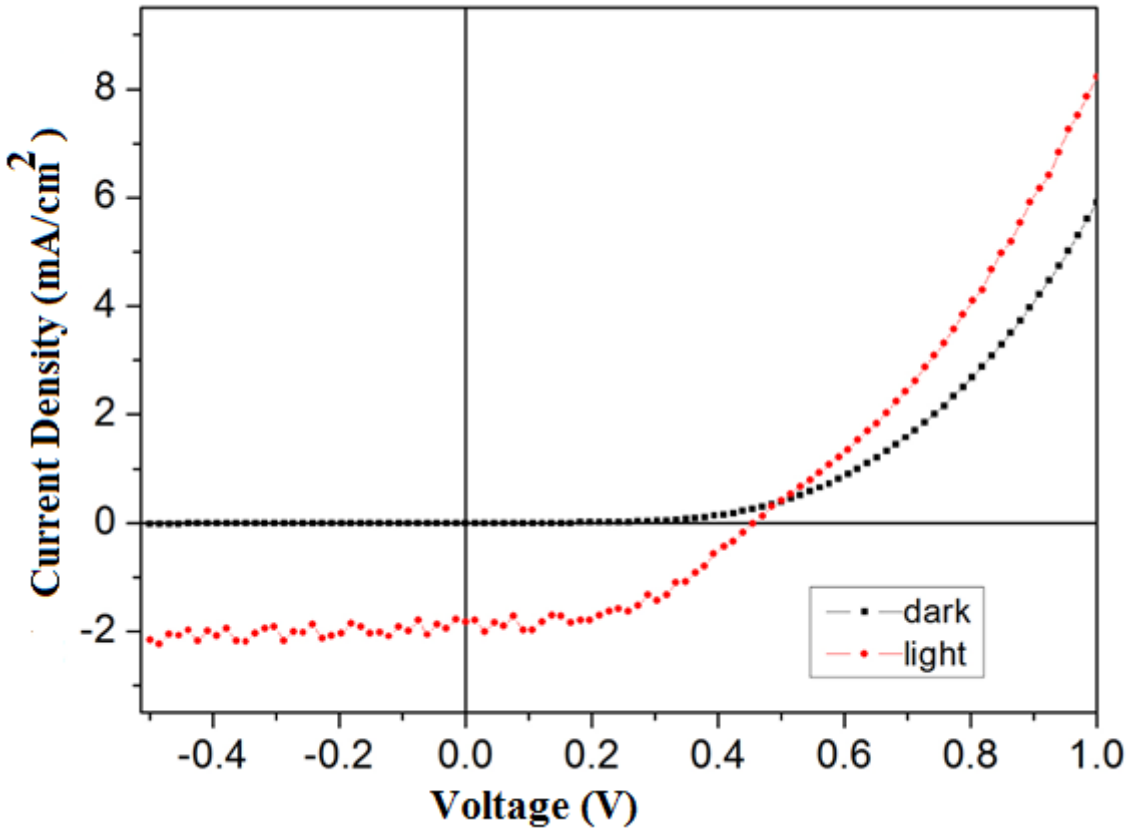

Figure 5.7: J-V plot for solar cell with device structure ITO|ZnO|P3HT:PC60BM|MoO3|Al

Table 5.3: Device parameters for device ITO|ZnO|P3HT:PCBM|MoO3|Al

Fill Factor (FF) (%)	**V_{OC} (V)**	**J_{SC} (mA/cm^2)**	**PCE (%)**
58.2	0.59	0.246	0.1

As seen in Fig. 5.7, the solar cell shows almost negligible shunt resistance and excellent fill factor (FF). The only downside is the current density values. They are very low. We have tried to increase it as mentioned before by using ZnO-polymer composite films as the electron transport layer (ETL). We will see that current density values increase exponentially

due to the composite films used. A possible reason for low current density values maybe the defects created in ZnO film during heat treatment and due to the low spatial distribution of ZnO nanoparticles.

Hence, we started thinking about making a composite of ZnO solution with cationic poly-electrolytes and chosen the well-known polymers such as- PVP and PAS.

In pure ZnO film the ZnO nanoclusters have non-homogenous arrangement and no proper connectivity exists between the nanoclusters (Fig. 5.8 (a)). On addition of the polymer, the clusters arrange into homogenous manner and the polymer strands bind the clusters together thus providing a suitable connecting path in between the nanoclusters (Fig.5.8 (b)). After addition of the polymer and spin coating it, the film needs to be heated at 200°C for 30 minutes.

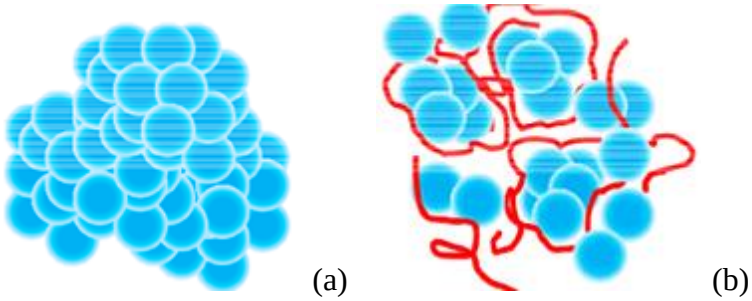

Figure 5.8: Arrangement of ZnO nanoclusters (a) before addition of polymer (b) after addition of polymer and heating [55].

5.2.2 Inverted device using ZnO-PAS

The first polymer tried in combination with ZnO was PAS or Poly(acrylic acid sodium). This ZnO-polymer composite prepared as explained in section 4.5, too gives us positive results but with very low current values (Fig. 5.9). Further optimization in thickness and concentration is required for this polymer.

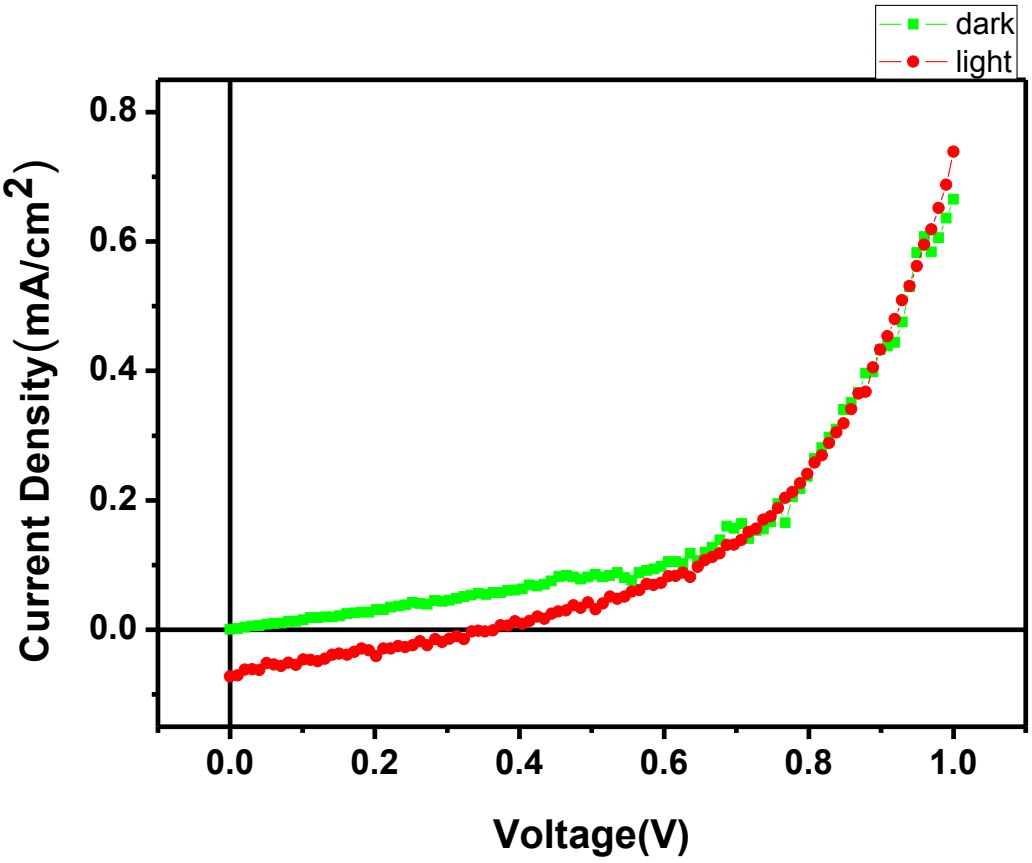

Figure 5.9: Dark and light characteristics of the device structure ITO|ZnO-PAS|P3HT:PCBM|MoO_3|Al.

Table 5.4 Device parameters for device ITO|ZnO-PAS|P3HT:PCBM|MoO_3|Al

Fill Factor (FF) (%)	**V_{OC} (V)**	**J_{SC} (mA/cm^2)**	**PCE (%)**
31.6	0.363	0.0723	0.01

5.2.3 Inverted device using ZnO-PVP

Secondly, the polymer tried and experimented in this category was a well known polymer PVP or Polyvinylpyrrolidone. The solution was prepared as per the section 4.5 and coated at 2000 rpm over the ITO substrate. It was then annealed at 200ºC for 30 minutes. The obtained results are as shown in the Fig.5.10 and device parameters are summarized in Table 5.5. It is obvious from the Fig.5.10 that the J-V characteristics of the devices based on ZnO-PVP as interfacial layer in inverted structure have better device characteristics and parameters with

respect to those based on ZnO only. The improvement in current and efficiency shows that the ZnO-PVP nanocomposite helps in reducing the series resistance and hence improves the device performance.

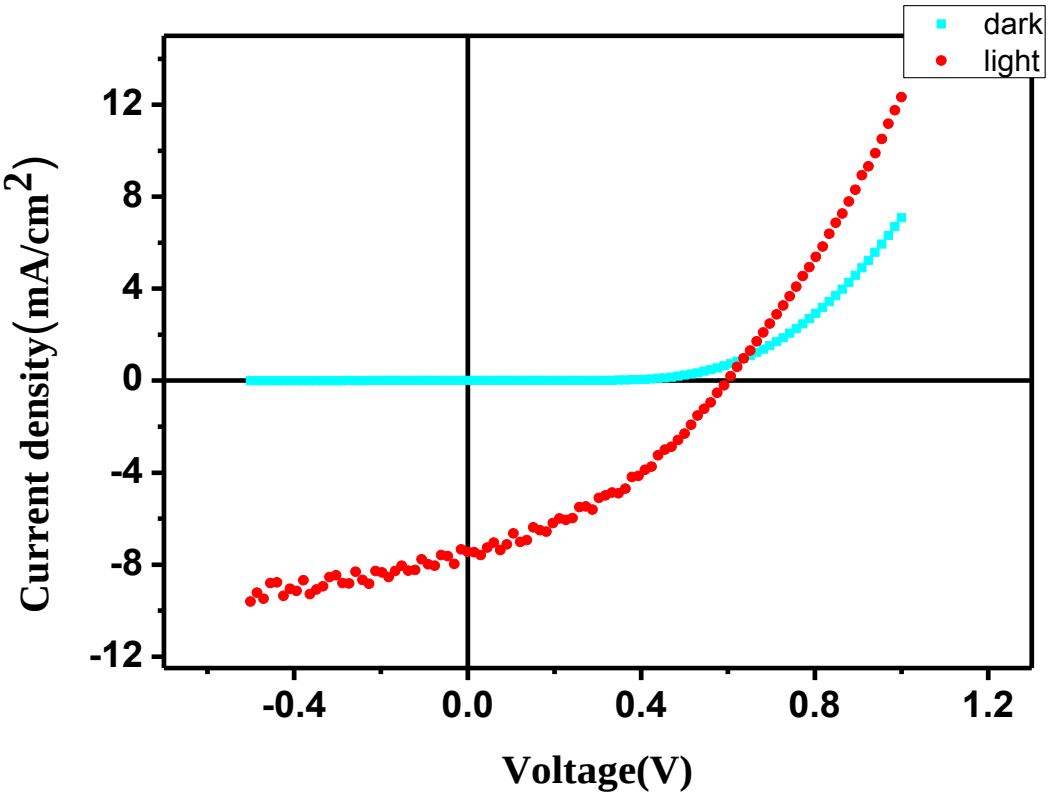

Figure 5.10: Dark and light characteristics of the device structure ITO|ZnO-PVP|P3HT:PCBM|MoO_3|Al.

Table 5.5 Device parameters for device ITO|ZnO-PVP|P3HT:PCBM|MoO_3|Al

Fill Factor (FF) (%)	**V_{OC} (V)**	**J_{SC} (mA/cm^2)**	**PCE (%)**
37.9	0.606	7.45	1.71

5.2.4 Inverted device using PFN

This is another inverted structured based device that employed the polymer named PFN or poly [(9,9-bis(3'-(N,N-dimethylamino)propyl)-2,7-fluorene)-alt-2,7-(9,9–dioctylfluorene). The J-V characteristics for different rpm's of PFN are as shown in Fig. 5.11.

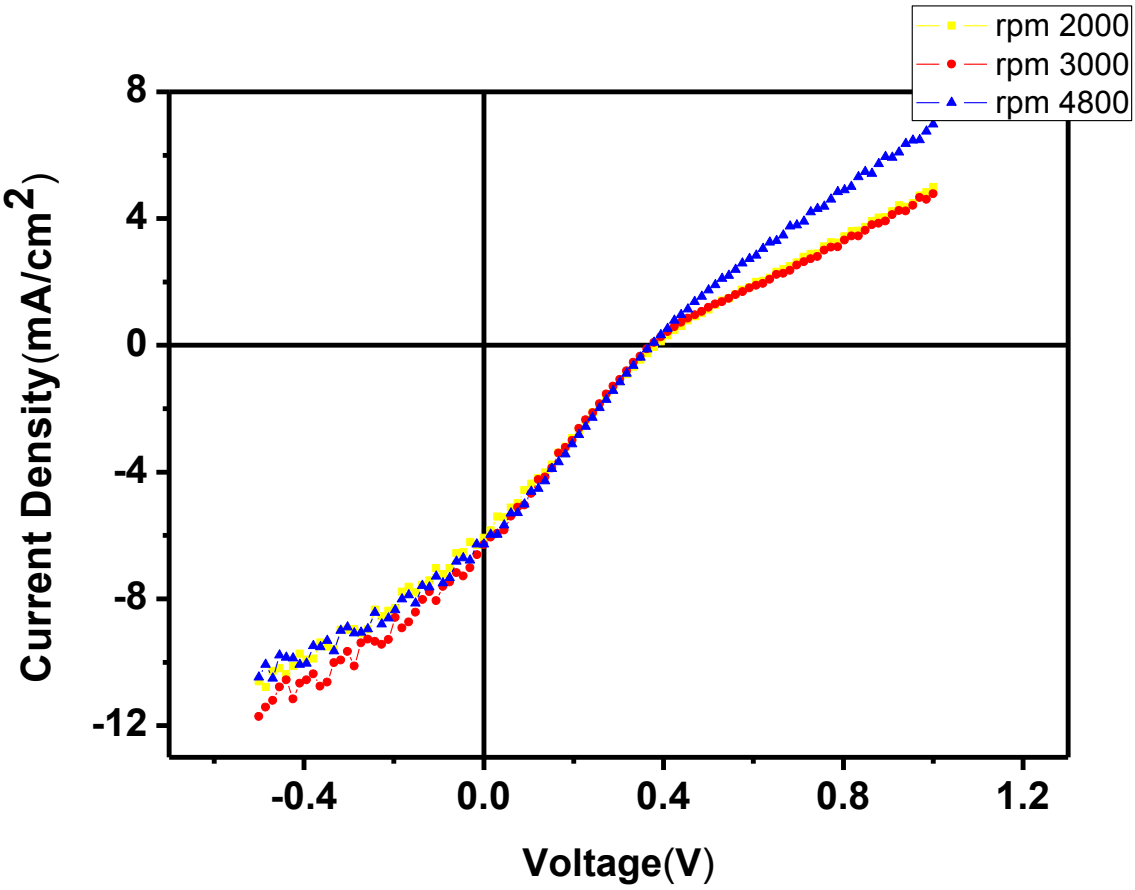

Figure 5.11: J-V characteristics of ITO|PFN|P3HT:PCBM|MoO_3|Al with different rpm

Table 5.6 Device parameters for device ITO|PFN|P3HT:PCBM|MoO_3|Al

Rotation speed	Fill Factor (FF) (%)	V_{OC} (V)	J_{SC} (mA/cm^2)	PCE (%)
2000	24.4	0.394	6.07	0.582
3000	24.8	0.379	6.29	0.591
4800	26.3	0.379	6.27	0.626

Effect of Post annealing on ITO|PFN|P3HT:PCBM|MoO_3|Al

It was observed that the inverted device using PFN showed much better results when the device was again annealed or post annealed after the complete fabrication. Once the aluminium deposition was over, the device was taken out for characterisation. And then, after obtaining the J-V plots, it was again kept for annealing at 120ºC for 20-25 minutes in air. This substantially increased the current and the efficiency of the cell as shown in Fig.5.12. The J_{SC} values before and after annealing were found to be 2.87mA and 6.41mA respectively.

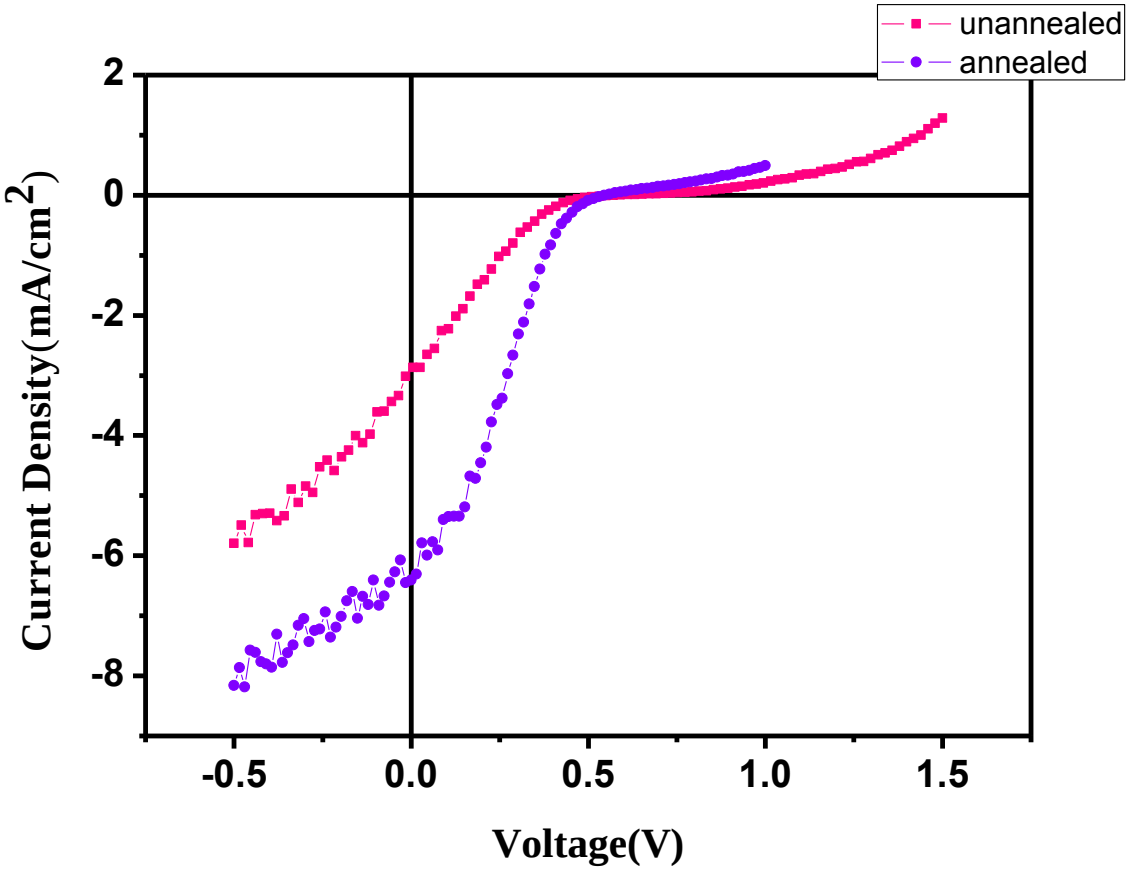

Figure 5.12: J-V characteristics for unannealed and annealed device structure ITO|PFN|P3HT:PCBM|MoO_3|Al

Optimized characteristics for PFN

After trying various combinations of the filter used, the rotation speed, and post annealing of the device, it was found the best results were observed when:

- A pvdf filter was used to filter PFN solution.
- The rpm taken for spin coating of the PFN solution was 4800.
- The device was post annealed at 120ºC for 20-25 minutes.

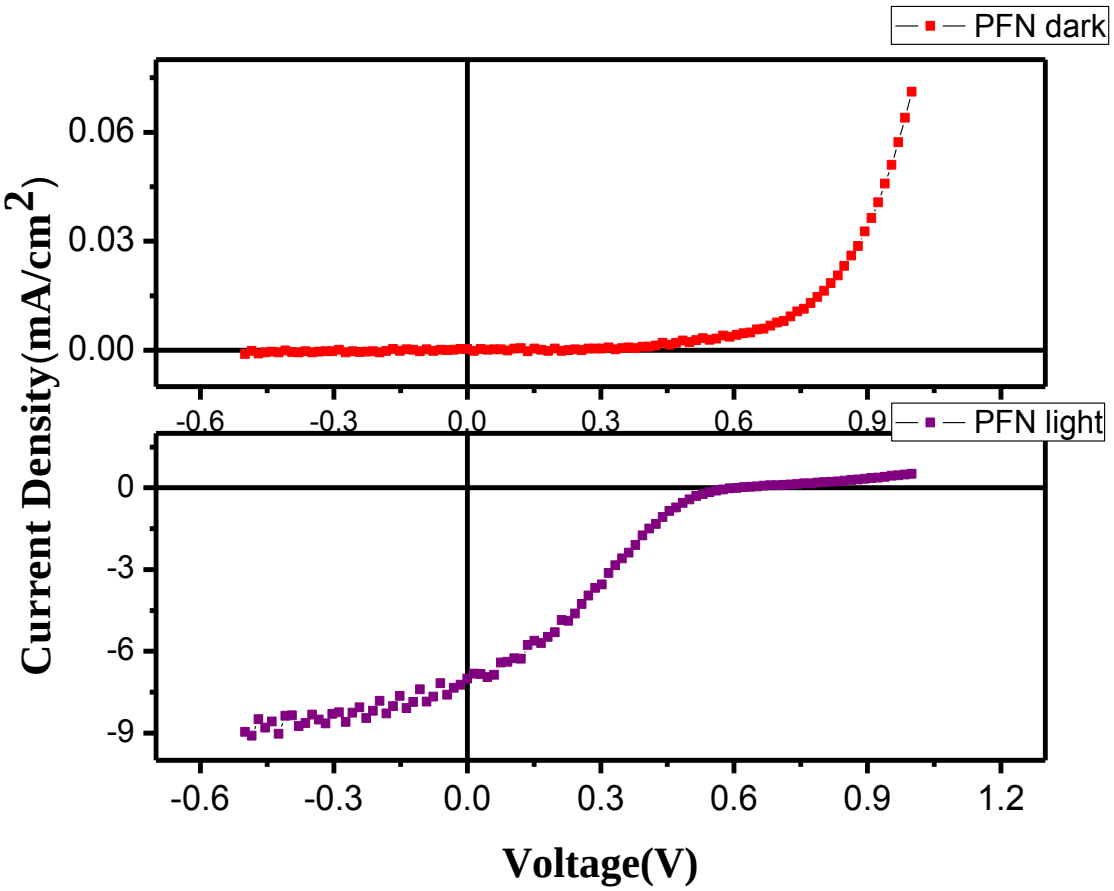

Figure 5.13: Light and dark characteristics for optimized structure ITO|PFN|P3HT:$PC_{60}BM$|MoO_3|Al.

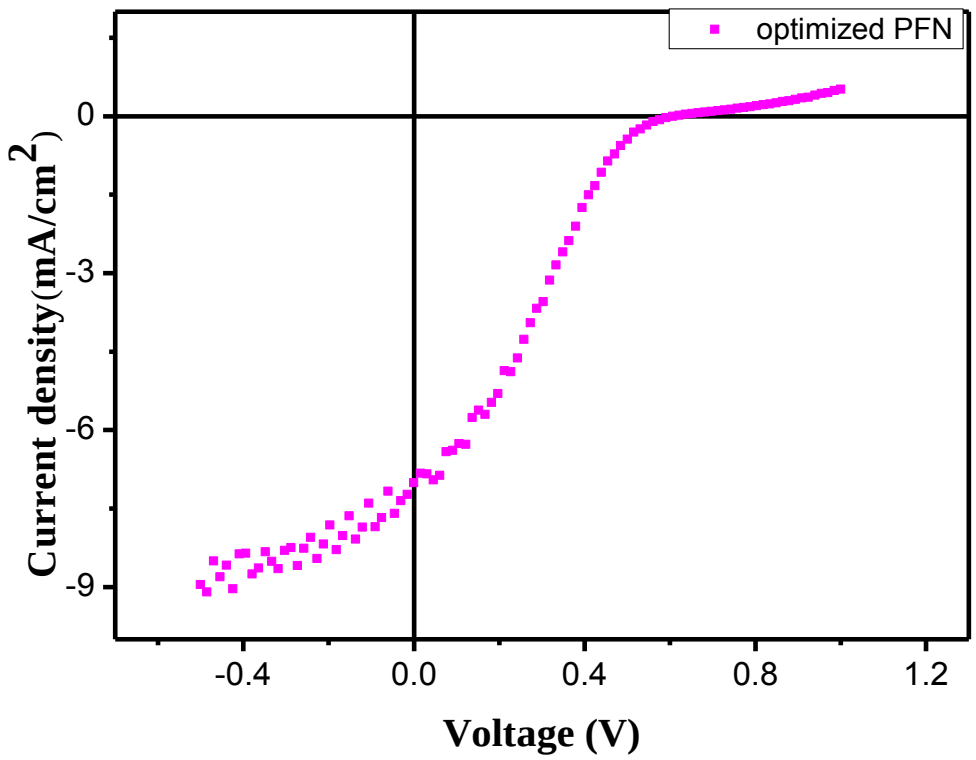

Figure 5.14: Optimized J-V plot for solar cell with device structure ITO|PFN|P3HT:$PC_{60}BM$|MoO_3|Al.

Table 5.5: Device parameters for solar cell with device structure ITO|PFN|P3HT:$PC_{60}BM$|MoO_3|Al.

FF (%)	V_{OC} (V)	J_{SC} (mA/cm^2)	PCE (%)
26.4	0.606	7.01	1.12

The device structure with PFN as interlayer showed efficiency as high as 1.12%. This structure paves way for a new combination for future scope and that is an interlayer of ZnO-PFN nanocomposite.

Out of all the structures fabricated, it is evident that inverted structures are much more efficient and stable. Moreover we were able to get rid of PEDOT:PSS and found that the device structures using various oxides (ZnO or MoO_3) prove out to be better alternatives. Further optimization and study of these structures can give some very promising results in future.

6. SUMMARY, CONCLUSION and FUTURE SCOPE

6.1 Summary of Results

In our investigation of organic solar cell we studied both conventional as well as inverted devices. The device structures investigated here are

- ITO/PEDOT:PSS/P3HT:PCBM/Al
- ITO/MoO_3/P3HT:PCBM/Al
- ITO/ZnO/P3HT:PCBM/Al
- ITO/ZnO-PAS/P3HT:PCBM/MoO_3/Al
- ITO/ZnO-PVP/P3HT:PCBM/MoO3/Al
- ITO/PFN/P3HT:PCBM/MoO3/Al

The combined results of the conventional structures are as in Fig. 6.1 below.

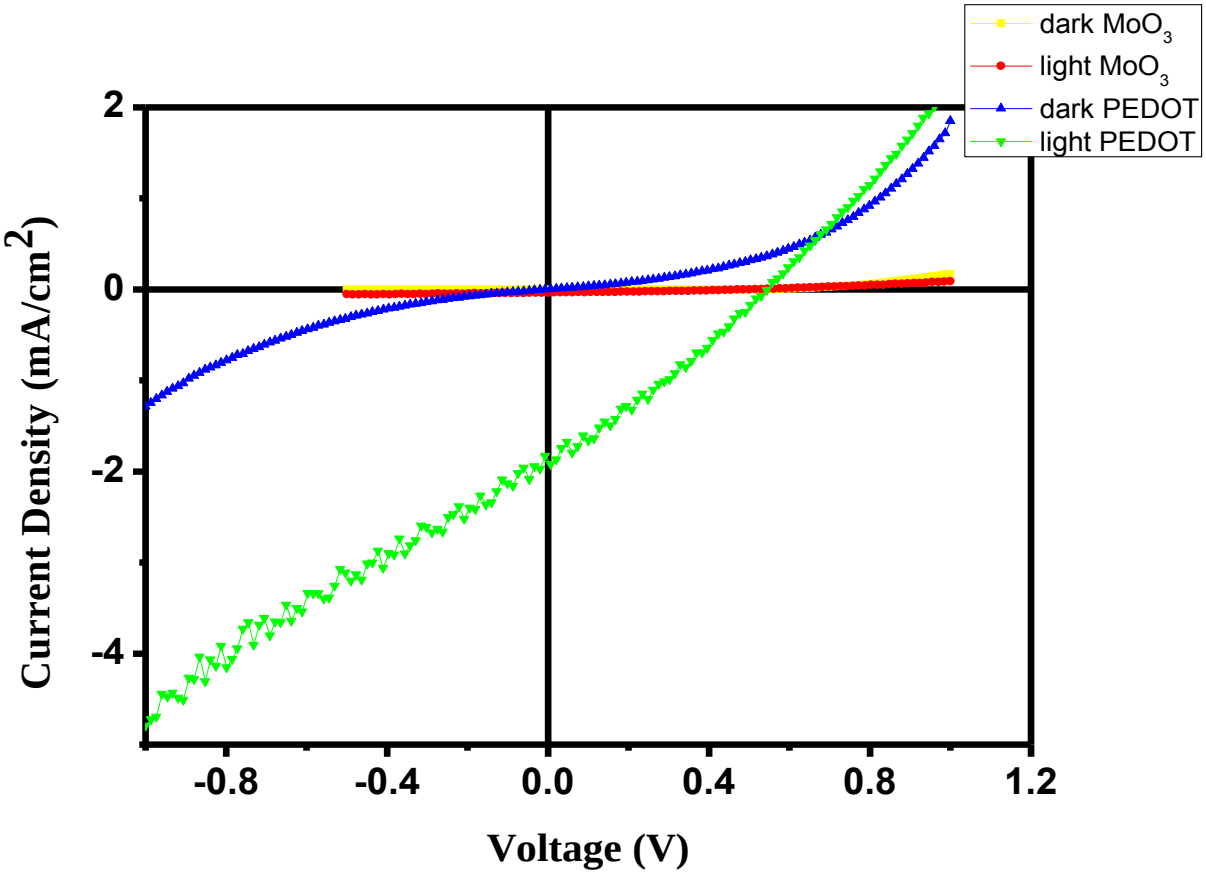

Figure 6.1: J-V plot for devices - ITO/PEDOT:PSS/P3HT:PCBM/Al and ITO/MoO3/P3HT:PCBM/Al

And the combined results for all the inverted systems fabricated are in figure 6.2

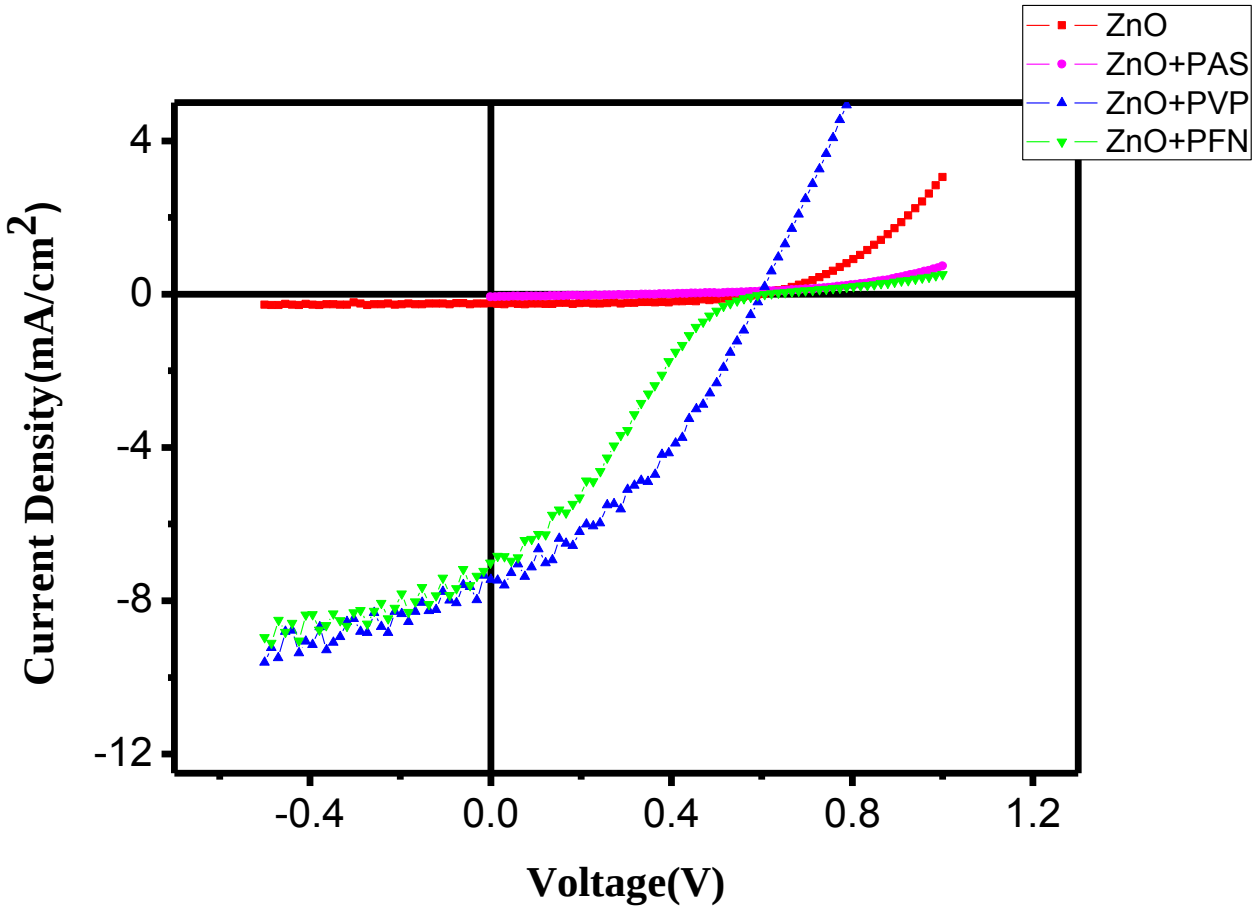

Figure 6.2: J-V plot for solar cell with device structure ITO|ZnO|P3HT:$PC_{60}BM$|MoO_3|Al; ITO|ZnO-PAS|P3HT:$PC_{60}BM$|MoO_3|Al; ITO|ZnO-PVP|P3HT:$PC_{60}BM$|MoO_3|Al and ITO|PFN|P3HT:$PC_{60}BM$|MoO_3|Al.

Fig. 6.1 shows the J-V characteristics of the conventional structure under AM1.5G solar irradiation. In these conventional structures we demonstrated that an efficient conventional solar cell can be fabricated using solution processed Molybdenum Oxide (MoO_3) as an anode inter facial layer. The J-V characteristics (Fig. 6.1) using solution processed MoO_3 shows better shape with respect to PEDOT:PSS. These results have been obtained in association with the work done by my colleague Mr. Sriraj Pillai with reference to his thesis work namely "Interface Layer Modification using polyelectrolytes for High Efficiency Organic Solar Cell".

However, further investigation and optimization are necessary in view of leakage current and durability concerns. The device leakage currents can be addressed by proper analysis of the interface of the devices using atomic force microscopic analysis.

Further the Fig. 6.2 represents the J-V plot of the inverted devices investigated in this report. As the figure points out that the device based on ZnO shows a typical open circuit voltage (V_{oc}) of 0.59V, short circuit current (J_{sc}) of 0.246 and fill factor of 52% showing a PCE value of 0.1%. However, when the PVP was added to ZnO to form ZnO-PVP nanocomposite then the V_{oc} remained same but, J_{sc} increases to 7.45mA/cm^2, achieving an efficiency of 1.7% which is 17 times higher than the value obtained for only ZnO based devices (Table 6.1). In one of the inverted devices we replaced ZnO by an alternative material PFN which also showed an improvement in the device parameters. However, this strategy needs more optimization in view of various compositions of ZnO and PFN. Moreover, one can also try the interface layer as the combination of ZnO-PFN nanocomposite too.

Table 6.1 Device parameters for the all the devices fabricated-

Conventional: ITO|PEDOT:PSS|P3HT:PCBM| and Al and ITO|MoO3|P3HT:PCBM|Al

Inverted: ITO|ZnO|P3HT:$PC_{60}BM$|MoO_3|Al; ITO|ZnO-PAS|P3HT:$PC_{60}BM$|MoO_3|Al; ITO|ZnO-PVP|P3HT:$PC_{60}BM$|MoO_3|Al and ITO|PFN|P3HT:$PC_{60}BM$|MoO_3|Al.

Interlayer	**FF (%)**	**V_{OC} (V)**	**J_{SC} (mA/cm^2)**	**PCE (%)**
PEDOT:PSS (1500rpm)	28	0.557	1.97	0.308
MoO_3 (2000rpm)	32.8	0.51	0.71	0.120
ZnO	58.2	0.59	0.246	0.10
ZnO-PAS	31.6	0.363	0.0723	0.01
ZnO-PVP	37.9	0.606	7.45	1.71
PFN	26.4	0.606	7.01	1.12

6.2 Conclusions and Future scope

This thesis met its primary objective by successfully demonstrating processes to synthesize and characterize P3HT:PCBM solar cells. The best efficiencies of the normal and inverted P3HT:PCBM solar cells, 0.3 % and 1.71 % respectively, were modest compared to high-performing inorganic photovoltaics, but not drastically different from the efficiencies of

P3HT:PCBM OPVs in the literature. Moreover, the conventional devices with MoO_3 as the buffer layer employed a complete solution route to the fabrication process which is a much more cost efficient approach as compared to the traditional techniques.

In the ZnO-only devices a typical open circuit voltage (V_{OC}) of 0.59V, short circuit current (J_{SC}) of 0.246 mA/cm^2 and fill factor of 58.2% achieved giving a PCE of 0.1%. When PVP was added to ZnO to obtain the nanocomposite layer, then the device exhibited improved performance with fill factor, V_{OC}, J_{SC}, and PCE 37.9, 0.606, 7.45 and 1.71 respectively (see Table 6.1). These values of device parameters showed superior interface properties of the ZnO-PVP nanocomposite. The improved electron collection capability of the ZnO-polymer nanocomposite may have resulted in better device parameters. Probably, the addition of PAS and PVP to ZnO solution works as an excellent surface smoothening material for ZnO planarization. This function may be similar to that of PEDOT:PSS smoothening ITO surfaces and reducing leakage current. Hence this kind of interlayer nanocomposite may be used to improve the device performance.

This gives rise to a new scope for the use of different polymers in combination with ZnO to make different nanocomposites in order to give high efficiency, high stability inverted structured devices. In this attempt, we tried the novel polymer PAS and PVP in combination with ZnO. Though the resultant parameters are needed to be optimized but the presence of the photo electric effect is in itself an achievement. These polymers not only improved the charge collection but also smoothened the ZnO surfaces, thereby reducing the leakage due to interfacial defects.

In this way, our study represents better device parameters of the inverted devices over the conventional ones. Though it needs a whole a lot of optimizations in terms of layer thickness, processing temperatures as well as various proportions taken for the buffer and active layers, still the results are promising.

Since organic solar cells hold great promise as a source of low cost, clean energy, the research conducted in this thesis should be continued and improved. More data and tests of the effect of encapsulation on device lifetimes are needed. In addition, more inverted cells should be fabricated and their stabilities should be monitored over several days. To get higher yields for normal and inverted devices, a more meticulous approach at understanding the reasons for OPV failure should be taken.

REFERENCES

1. National Oceanic US Department of Commerce and Atmospheric demonstration. Trends in carbon dioxide. Earth System Research Laboratory, 2010.
2. B. Mc Kibben. The tipping point. Yale Environment 360, June 3 2008.
3. US Energy Information Administration. Independent Statistics and Analysis, August http://www.eia.doe.gov/cneaf/alternate/page/renewenergyconsump/rea prereport.html 2010.
4. M. M. Wienk, M. G. R. Turbiez, M. P. Struijk, M. Fonrodona and R. A. J. Janssen, Appl. Phys. Lett., 88: 153511-514, 2006.
5. F. C. Krebs. Polymeric Solar Cells: Materials, Design, Manufacture. DEStech Publications, Inc., Lancaster, Pennsylvania, 2010.
6. W. Shockley and H. J. Queisser. Appl. Phys, 32: 510-519, 1961.
7. M. J. Kerr, A. Cuevas, and P. Campbell. Progress in Photovoltaics: Research and Applications, 11: 97-104, 2003.
8. M. A. Green, K. Emery, Y. Hishikawa, and W. Warta. Solar cell efficiency tables (version 36). Progress in Photovoltaics: Research and Applications, 18: 346-352, 2010.
9. Solarbuzz. September URL:http://www.solarbuzz.com/index.asp,2010.
10. S. E. Shaheen, D. S. Ginley, and G. E. Jabbour. MRS Bulletin, 30: 10-19, January 2006.
11. Z. He, C. Zhong, S. Su, M. Xu, et al, Nature Photonics, 6: 591–595, 2012
12. F.C. Krebs. Polymer Photovoltaics, A Practical Approach, SPIE Press, Bellingham, Washington, 2008.
13. M. LoCascio. Application of semiconductor nanocrystals to photovoltaic energy conversion devices, 2002
14. L. Kazmersk. Best research solar cells efficiencies, http://www.nrel.gov/pv/, 2010.
15. S. Genes, H. Neugebauer, and S. N. Sariciftci, Chemical Reviews, 107: 1324-1338. 2007
16. http://www.iea.org/publications/freepublications/publication/renewable factsheet.pdf 2007
17. Y. Yuan, J. Huang and G. Li, Green, 1: 65–80, 2011
18. F. C. Krebs. Solar Energy Materials and Solar Cells, 93: 465 -475, 2009.
19. R. Gaudiana, C. J. Brabec, Nature Photonics 2: 287–289, 2008.
20. W. Cai, X. Gong, Y. Cao. Solar Energy Materials & Solar Cells 94: 114–127, 2010
21. B. O'Regan, M. Grätzel, Nature 335: 737-739, 1991
22. M. K. Nazeeruddin, P. Réchy, T. Renouard, et al., J. Am. Chem. Soc. 123: 1613-1624, 2011.

23. Introduction to polymer solar cells (3Y280) René Janssen, http://faculty.mu.edu.sa/public/uploads/1339275819.829Polymer%20solar%20cells.pdf
24. G. A. Chamberlain, Organic Solar Cells- A Review, 8: 47-83, 1983
25. N. S. Sariciftci (Ed.), Primary photoexcitations in conjugated polymers: Molecular Exciton versus Semiconductor Band Model, World Scientific Publishers, Singapore, 1998.
26. G. Yu, Y. Gao, J. C. Hummelen, F. Wudl and A. J. Heeger, Sc. 270: 1789-1791, 1995.
27. E. Klimov, W. Li, X. Yang et al. Macromolecules, 39: 4493-4496, 2006.
28. M. Jørgensen, K. Norrman, F.C. Krebs, Sol. Energy Mater. Sol. Cells 92: 686–714, 2008.
29. F.C. Krebs, K. Norrman, Prog. Photovolt.: Res. Appl. 15: 697–712, 2007.
30. K. Takanezawa, K. Tajima, K. Hashimoto, Appl. Phys. Lett. 93: 063308(1- 3), 2008.
31. P. W. M. Blom, V. D. Mihailetchi, L. J. A. Koster, D. E. Markov, Adv. Mater. 2007.
32. http://en.wikipedia.org/wiki/Exciton.
33. A. Haugeneder, M. Neges, C. Kallinger, et al. Phys. Rev. B, 59: 15346-15352, 1999.
34. L. A. A. Pettersson, L. S. Roman, O. Inganäs, J. Appl. Phys. Lett. 86: 487-496, 1999.
35. H. B. Michaelson, Applied Physics, 48: 4729–4733, 1977.
36. J. M. Bharathan and Y. Yang, Journal of Applied Physics, 84: 3207–3211, 1998.
37. Y. Park, V. Choong, E. Ettedgui, et al., Applied Physics Letters, 69: 1080–1082, 1996.
38. E. Aminaka, T. Tsutsui and S. Saito, J. Appl. Phys., 79: 8808-8816, 1996
39. S. A. Van Slyke, C. H. Chen, C. W. Tang, Appl. Phys. Lett. 69: 2160-2163, 1996
40. N. Sahu, B Parija and S Panigrahi, Indian J. Phys., 83: 493-502, 2009
41. Y. Kim, A. M. Ballantyneb, J. Nelsonb and D. D.C. Bradley. Elseiver, Organic Electronics, 205, Feb 2009
42. J. preet, A.J. Heeger, G.C. Bazan, Acc. Chem. Res. 42: 1700-1708, 2009
43. F.C. Krebs, Sol. Energy Mater. Sol. Cells. 93: 465-475, 2009
44. C. E. Small, S. Chen, J. Subbiah, C. M. Amb, S-W Tsang, T.Z Lai, J. R. Reynolds, F. So, Nature Photonics, 6: 115-120, 2012.
45. T. Du, H. Song, O. J. Ilegbusi. Materials Science and Engineering: C, 2(3), 414–420, 2007
46. B.-S. Kim, D.-E. Kim, Y.-K Jang, et al., Journal of the Korean Physical Society, 50: 1858, 2007
47. H. W. Heuer, R. Wehrmann, and S. Kirchmeyer, Adv. Funct. Mater. , 12, 89, 2002
48. H. K. Lee, J. H. Seo, Y. K. Kim et al., J. Korean Phys. Soc., 49, 1052-1056, 2006
49. J. Y. Kim, J. H. Jung, D. E. Lee, and J. Joo, Synth. Mat. 126: 311-316, 2002

50. Y. Sun, J.H. Seo, C.J. Takacs, J. Seifter, A.J. Heeger, Advanced Materials, 23: 1679-1683, 2011
51. Key World Energy Statistics, International Energy Agency, 2012
52. Justin Gillis, Heat-Trapping Gas Passes Milestone, Raising Fears, The New York Times, May 2013
53. J. You, C. C. Chen, L. Dou et al., Adv. Mater, 24: 5267-5272, 2012
54. H. Cheung, C. Fuentes-Hernandez, Y. Zhou, et al., The Journal of Physical Chemistry, 114: 20713-20718, 2010
55. T. Hu, F. Li, K. Yuan and Y. Chen, ACS Applied Materials and Interfaces, 5: 5763-5770, 2013

THANK YOU…